Rotenone and elevated extracellular potassium concentration induce cell-specific fibrillation of α-synuclein in axons of cholinergic enteric neurons in the guinea-pig ileum

by

DF Sharrad[1], BN Chen[1], WP Gai[1], N Vaikath[2], OM El-Agnaf[2], SJH Brookes[1]

1. Discipline of Human Physiology, FMST, School of Medicine, Flinders University, Bedford Park, South Australia 5042

2. Neurological Disorders Center, Qatar Biomedical Research Institute, and College of Science and Engineering, Hamad Bin Khalifa University (HBKU), Education City, Qatar Foundation, P.O. Box 5825, Doha, Qatar.

Address for Correspondence

Simon Brookes, simon.brookes@flinders.edu.au,

Tel: +61 8 8204 4201; Fax: +61 8 8204 5768

Discipline of Human Physiology, FMST, School of Medicine

Flinders University, Sturt Road, Bedford Park, SA 5042

Running Title: High potassium concentration and rotenone promote aggregation of α-synuclein in the enteric nervous system

Abbreviations: ChAT, choline acetyltransferase; GI, gastrointestinal; K+, potassium; NOS, nitric oxide synthase; SNARE, soluble *N*-ethylmaleimide-sensitive factor activating protein receptor; SNpc, substantia nigra pars compacta; VAChT, vesicular acetylcholine transporter

Word count: 4480

ABSTRACT

Background: Parkinson's disease is a progressive neurodegenerative disorder that results in the widespread loss of select classes of neurons throughout the nervous system. The pathological hallmarks of Parkinson's disease are Lewy bodies and neurites, of which α-synuclein fibrils are the major component. α-Synuclein aggregation has been reported in the gut of Parkinson's disease patients, even up to a decade before motor symptoms, and similar observations have been made in animal models of disease. However, unlike the central nervous system, the nature of α-synuclein species that form these aggregates and the classes of neurons affected in the gut are unclear. We have previously reported selective expression of α-synuclein in cholinergic neurons in the gut (1), suggesting they may be particularly vulnerable to degeneration in Parkinson's disease.

Methods: In this study, we used immunohistochemistry to detect α-synuclein oligomers and fibrils via conformation-specific antibodies after rotenone treatment or prolonged exposure to high [K+] in *ex vivo* segments of guinea-pig ileum maintained in organotypic culture.

Key Results: Rotenone and prolonged raising of [K+] caused accumulation of α-synuclein fibrils in the axons of cholinergic enteric neurons. This took place in a time- and, in the case of rotenone, concentration-dependent manner. Rotenone also caused selective necrosis, indicated by increased cellular autofluorescence, of cholinergic enteric neurons, labeled by ChAT-immunoreactivity, also in a concentration-dependent manner.

Conclusions & Inferences: To our knowledge, this is the first report of rotenone causing selective loss of a neurochemical class in the enteric nervous system. Cholinergic enteric

neurons may be particularly susceptible to Lewy pathology and degeneration in Parkinson's disease.

KEY MESSAGES

- Constipation is a common complaint in Parkinson's disease. Selective neuronal vulnerability is a hallmark of the disease; however, whether select classes of enteric neurons are particularly vulnerable to degeneration in the disease is unclear.

- Here, we show that rotenone, a pesticide implicated in Parkinson's disease, and elevated potassium cause accumulation of α-synuclein, a key feature of Parkinson's disease, in cholinergic enteric neurons.

- Enteric cholinergic neurons may be particularly vulnerable to degeneration in Parkinson's disease, which may underlie constipation.

INTRODUCTION

Parkinson's disease is a progressive neurodegenerative disorder characterized by the widespread loss of select classes of neurons throughout the nervous system. The pathological hallmarks of sporadic Parkinson's disease are Lewy bodies and neurites: abnormal protein aggregates found in surviving nerve cell bodies and axons at sites of neurodegeneration, of which the presynaptic protein, α-synuclein, is the major constituent (2, 3, 4). Many structures outside of the substantia nigra pars compacta (SNpc) are damaged by the disease (5) and there is now strong evidence that sporadic Parkinson's disease starts at a remote site before spreading to the SNpc (6, 7). Putative sites of initiation are regions in the periphery connected

to the brainstem, including the olfactory mucosa and gastrointestinal (GI) tract (8). Although Parkinson's disease is best known for its characteristic motor symptoms, non-motor symptoms impose a significant burden on quality of life (10, 11). These arise early in the course of disease and are often unresponsive to, or worsened by, dopamine-replacement therapy (11, 12). The dominance of non-motor symptoms in the pre-clinical stages of disease has helped guide the quest for biomarkers that can provide an accurate diagnosis before the onset of motor symptoms. For this reason, much attention has been focused on the GI tract, which is heavily burdened by Lewy pathology (13) and commonly expresses symptoms including dysphagia, bloating and constipation (14). Of these, constipation has been reported to manifest as early as 10 years prior to motor symptoms (15). Curiously, accumulation of α-synuclein can occur in the gut up to 10 years prior to diagnosis (16). The gut's putative role in the pathogenesis of Parkinson's disease and its accessibility makes it suitable for investigating mechanisms underlying disease pathogenesis and assessing efficacy of disease-modifying agents and candidate disease biomarkers. Aggregation of α-synuclein is central to these goals. Mutations in *SNCA*, the gene encoding α-synuclein, as well as gene duplications and triplications, which increase its propensity to aggregate, can cause Parkinson's disease (17). α-Synuclein oligomers are elevated in the cerebrospinal fluid in Parkinson's disease (18,19) and can seed the aggregation of endogenous α-synuclein in both central (20) and peripheral (21, 22) neurons. Although the mechanisms are not entirely clear, mitochondrial dysfunction and oxidative stress may contribute to aggregation of α-synuclein in Parkinson's disease (23). There is a positive relationship between exposure to the pesticide rotenone and risk of Parkinson's disease (24), and biochemical studies implicate a systemic defect in mitochondrial complex I (25). Rotenone is a mitochondrial complex I inhibitor capable of replicating the classic features of Parkinson's disease, thereby demonstrating a direct link between mitochondrial dysfunction and α-synuclein aggregation (26, 27). Metabolic stress

evoked by elevated intracellular calcium concentration provoked by raised extracellular potassium concentration can also induce α-synuclein aggregation (28). Accordingly, the disease selectively targets highly metabolically active populations of neurons, but spares those that express high levels of calcium binding proteins (29).

In this study, we used immunohistochemistry to determine whether rotenone or prolonged exposure to raised [K+] in organotypic culture triggers accumulation of α-synuclein in the cell bodies and axons of enteric neurons in the guinea-pig ileum. We used a conventional antibody against α-synuclein in addition to novel conformation-specific antibodies against α-synuclein oligomers and fibrils (30).

MATERIALS AND METHODS

Guinea-pig tissue collection

Adult guinea-pigs of either sex (weight 230–400g) were stunned and killed by exsanguination, in a manner approved by the Animal Welfare Committee of Flinders University, South Australia. Animals were opened along the ventral midline and the ileum with mesentery attached was removed, intestinal contents were flushed and the preparation placed in Krebs solution (118mM NaCl, 4.75 mM KCl, 1.0mM NaH_2PO_4, 25 mM $NaHCO_3$, 1.2mM $MgSO_4$, 11.1 mM D-glucose, 2.5mM $CaCl_2$, bubbled with 95%O_2/5%CO_2). Tissue was pinned in a Sylgard-lined Petri dish (Dow Corning, Midland, MI) and the gut was opened longitudinally alongside the mesenteric border. The mucosa and submucosa were carefully removed via sharp dissection and discarded and the remaining preparation was pinned circular muscle-side up. Krebs solution was changed regularly during dissection.

Organotypic culture

Tissue was kept alive in an organotypic culture in medium [Dulbecco's modified Eagle's/Ham's F12, Sigma (1: 1 ratio mix, supplemented with L-glutamine and 15 mmol L^{-1} hydroxyethyl piperazineethanesulfonic acid (HEPES))]; including 10% fetal bovine serum, 1.8 mmol L^{-1} $CaCl_2$, 100 IU mL^{-1} penicillin, 100 μg mL^{-1} streptomycin D, 2.5 μg mL^{-1} amphotericin B, 20 g mL^{-1} gentamycin, Cytosystems, Castle Hill, Australia) for either 1, 2 or 4 days of culture. Rotenone was prepared in 100% DMSO as 0.1M solution and KCl was prepared as a 1M stock in distilled water. Tissue was maintained in organotypic culture in one of four serum-supplemented DME/F12 solutions containing: 10μM rotenone (final DMSO concentration of 0.01%); 1μM rotenone (final DMSO concentration of 0.001%); 10mM KCl; and standard medium (final DMSO concentration of 0.01%). Previous studies have demonstrated that DMSO concentrations at and below those used in the present study lack pharmacological activity (31). In addition, a specimen of tissue was taken from each animal immediately after euthanasia, maximally stretched and fixed immediately in modified Zamboni's fixative (2% formaldehyde, 15% saturated picric acid in 0.1M phosphate buffer, pH 7.0) for approximately 24 hours at 4°C. After 1, 2 or 4 days in culture, preparations were maximally stretched and fixed as above. Tissue was then cleared with three washes of 100% dimethylsulphoxide (DMSO), and stored in PBS at 4°C. For immunohistochemical labeling of myenteric ganglia, the circular muscle layer was removed by sharp dissection prior to incubation in antisera.

Immunohistochemistry

Preparations of myenteric plexus and longitudinal muscle, or strips of circular muscle, were cut into pieces approximately 10mm x 10mm and incubated with antisera against different combinations of markers (Table 1) at room temperature for two days. Preparations were rinsed three times in PBS and incubated with secondary antisera (Table 2) for 4 hours at room temperature. After a final rinse with PBS, preparations were equilibrated with 50%, 70%, and 100% carbonate-buffered glycerol, and mounted in 100% carbonate-buffered glycerol (pH 8.6). All antibodies were diluted in 0.1 M PBS (0.3 M NaCl) containing 0.1% sodium azide. Controls for double-labeling were performed by omitting one or more primary antibodies from the procedure, and by ensuring that all combinations of primary and secondary antisera were free of cross-reactivity.

Antibody characterisation

Syn-O1

The Syn-O1 antibody was a monoclonal raised in mice against α-synuclein fibrils (30). The antibody selectively binds α-synuclein oligomers and fibrils and not α-synuclein monomers on inhibition ELISA and dot blotting (30). When α-synuclein oligomers, protofibrils and fibrils were blotted on a nitrocellulose membrane, Syn-O1 detected all three conformations, but showed greatest immunoreactivity for fibrillar α-synuclein (30). Preabsorption of Syn-O1 with α-synuclein fibrils completely abolished its ability to detect α-synuclein fibrils, whereas preabsorption with α-synuclein monomers had little effect on its immunoreactivity (30). On a nitrocellulose membrane, the Syn-O1 antibody did not recognize monomers or fibrils generated from β- or γ-synuclein, or the fibrillar forms of other amyloidogenic proteins including Aβ, Tau_{40}, IAPP or ABri (30).

Syn-F2

The Syn-F2 antibody was a monoclonal raised in mice against α-synuclein fibrils (30). The antibody selectively binds α-synuclein fibrils and not α-synuclein monomers on inhibition ELISA and dot blotting (30). When α-synuclein oligomers, protofibrils and fibrils were blotted on a nitrocellulose membrane, Syn-F2 did not detect oligomers, had low immunoreactivity for protofibrils, but showed strong immunoreactivity for fibrillar α-synuclein (30). Preabsorption of Syn-F2 with α-synuclein fibrils completely abolished its ability to detect α-synuclein fibrils, whereas preabsorption with α-synuclein monomers had little effect on its immunoreactivity (30). On a nitrocellulose membrane, the Syn-F2 antibody did not recognize monomers or the fibrils generated from β- or γ-synuclein, or the fibrillar forms of other amyloidogenic proteins including Aβ, Tau_{40}, IAPP or ABri (30).

Microscopy, image analysis and processing

Specimens of fresh-fixed and organ-cultured tissue cultured were examined on an Olympus IX71 microscope (Japan) equipped with epifluorescence and highly discriminating filters (Chroma Technology Co., Battledore, VT). Images were captured using a Roper scientific (Coolsnap) camera at 1392 x 1080 pixels, using AnalySIS Imager 5.0 (Olympus-SIS, Münster, Germany) and saved as TIFF files. Micrographs of autofluorescent and immunohistochemically-labeled nerve structures were captured using a 40x objective water-immersion lens and displayed in ImageJ (NIH, Bethesda, MD). The identify of the preparations was concealed from the microscopist prior to analysis and several sampling techniques were utilized.

We quantified nerve cell bodies and abnormally large varicosities labeled by the conventional antibody against α-synuclein as follows. Images were taken of 30 randomly selected areas of tertiary plexus and 20 randomly selected myenteric ganglia by blindly moving the microscope stage to a new randomly selected area on the slide, then imaging the closest myenteric ganglion or area of tertiary plexus. The coordinates of each image were recorded to ensure the same area was never imaged twice. The number of cell bodies and abnormally large varicosities in each image were then counted. Totals were obtained in each of four guinea-pigs. The same methodology was used to obtain images of myenteric ganglia and tertiary plexus and to quantify the number of neural structures labeled with antisera against α-synuclein oligomers or α-synuclein fibrils.

In preparations that had not been labeled with antisera, dim, autofluorescent nerve cell bodies could be detected under all filter combinations (AMCA, FITC, Cy3 and Cy5). However, these were most prominent under the FITC filter set. When these preparations were subsequently labeled with antisera for ChAT (Cy5 fluorophore) and NOS (Cy3 fluorophore), this autofluorescence could no longer be detected in either Cy3 or Cy5 channels, presumable because labeling increased the background and swamped the dim autofluorescent signal. However, the autofluorescence remained visible in the FITC channel. This made it possible to determine the presence of ChAT- and NOS-immunoreactivity in autofluorescent nerve cell bodies.

Data collected from varicosity and cell body counts were rescaled for each animal using the following equation: $x' = x - min\ (x) / max\ (x) - min\ (x)$, where x' is the normalised value, x is the original count, $min\ (x)$ is the minimum value counted for that animal, and $max\ (x)$ is the maximum value counted for that animal. The mean number of cell bodies or varicosities

immunoreactive for a particular marker was calculated by generating an average of the normalised counts generated from each of the four animals. Group data were expressed as percentage means ± standard error of the mean (SEM), with n referring to the number of animals. The average total number of autofluorescent cell bodies was expressed as the mean of the total number of cells ± SEM, with n referring to the number of animals.

Fluorescence micrographs were prepared with Adobe Photoshop CS5 (San Jose, CA). Figures were generated from grayscale images adjusted for contrast and brightness and were cropped and resized, but no other digital processing was used.

Statistical analysis

One-way analysis of variance (ANOVA) with Tukey's HSD Test in SPSS19 for PC (SPSS, Chicago, IL) was used to compare the means of more than two samples. The means of two samples were compared by a Student's unpaired *t*-test in Microsoft Excel 2008 for Mac (Microsoft, Santa Rosa, CA). Differences were considered significant at $P < 0.05$.

RESULTS

Accumulation of α-synuclein in axons and cell bodies during organotypic culture

The tertiary plexus contains the axons of inhibitory nitrergic motorneurons and more abundant excitatory cholinergic motorneurons, which supply the overlying longitudinal muscle layers. Previous studies have shown that α-synuclein is expressed in the axons of all cholinergic motorneurons, identifiable by immunoreactivity for vesicular acetylcholine

transporter (VAChT), and is not expressed in the axons of nitrergic motorneurons, identified by immunoreactivity for NOS (33).

When guinea-pig ileum was maintained in organ culture, abnormally large varicosities were visible in the tertiary plexus after immunolabeling with the conventional antibody against α-synuclein (Figure 1). On average, their surface area was seven times greater than that of randomly sampled normal varicosities (Table 3). An observer, blinded to the tissue treatment, quantified these abnormally large varicosities in the tertiary plexus that were labeled by the conventional α-synuclein antibody from preparations cultured in each of the four solutions (Table 4). Total numbers of abnormally large α-synuclein varicosities varied considerably but they were consistently absent in all preparations that were fixed immediately after removal from the animal. Large varicosities were seen in all preparations subjected to organ culture, including those in standard DME/F12 medium without either rotenone or KCl. In most cases, large varicosities appeared by day 1, reached peak numbers by day 2, and reduced again by day 4 (Table 4). With 10μM rotenone, the peak number of large varicosities in the tertiary plexus appeared at day 4, but this did not reach significance ($P > 0.05$ in all instances, $f = 2.624$, $df = 11$). Similar abnormally large α-synuclein varicosities were also visible in the circular muscle and probably in the myenteric plexus, but could not be quantified for technical reasons. This suggests that the process of maintaining tissue in organ culture causes a small subset of varicosities to swell significantly, and this was not significantly affected by either rotenone or raised KCl.

Using the same conventional antibody to α-synuclein, we have previously reported that α-synuclein-immunoreactivity is not detectable in myenteric nerve cell bodies of the guinea-pig ileum fixed immediately after removal from the animal (33), although it is abundant in axons.

This was confirmed in the present study and extended by the observation that no detectable accumulation of α-synuclein was detectable in enteric nerve cell bodies after 1-4 days of organ culture in standard medium, 1μM or 10μM rotenone, or in medium supplemented with 10mM KCl.

Characterisation of antibodies against α-synuclein oligomers and fibrils

Aggregation of α-synuclein in nerve terminals and cell bodies is strongly implicated in the pathogenesis of Parkinson's disease. We used novel conformation-specific antibodies against α-synuclein fibrils and oligomers to detect these species in guinea-pig myenteric neurons after organotypic culture with and without rotenone and KCl (30). Control preparations of myenteric plexus were fixed immediately after removal from the animal and then processed for immunohistochemistry with a range of concentrations of antisera to α-synuclein fibrils (Syn-F2) and α-synuclein oligomers (Syn-O1). Both antibodies produced labeling of varicosities in myenteric ganglia, internodal strands, circular muscle plexus and tertiary plexus, but did not label enteric nerve cell bodies or inter-varicose fibres (Figure 2). This pattern was identical to previous reports using the conventional antibody to α-synuclein (29). We then identified a dilution threshold, below which labeling of varicosities in fresh-fixed tissue disappeared. The threshold dilution for these antibodies was: Syn-F2 (1:200) and Syn-O1 (1:1500). These threshold dilutions were then used to identify whether expression levels of their specific antigens (oligomers or fibrils) had increased above baseline under different conditions of organotypic culture.

Accumulation of α-synuclein fibrils in axons during organotypic culture

α-Synuclein fibrils could not be detected in axons or cell bodies in the myenteric plexus, tertiary plexus or circular muscle plexus in fresh-fixed preparations, using the threshold concentration of 1:200. Nor was labeling detectable after 1 and 2 days culture in standard DME/F12 medium (Figure 3). After 4 days of culture very weak and diffuse labeling was detected in the tertiary plexus in 1 of 4 preparations (Figure 3). In contrast, in DME/F12 with 1μM rotenone (Figure 4), 10μM rotenone (Figure 5), or 10mM KCl (Figure 6), α-synuclein fibrils could be readily detected in axons in the myenteric plexus, tertiary plexus and circular muscle plexus in 4 out of 4 preparations at 1, 2 and 4 days. In the first 2 days, α-synuclein fibrils were more abundant in the tertiary plexus than in the myenteric plexus, but by 4 days this difference had disappeared (Figures 4, 5 and 6). No accumulation of α-synuclein fibrils in myenteric nerve cell bodies was detected under any of the conditions tested.

Accumulation of α-synuclein oligomers in axons during organotypic culture

After 1, 2 or 4 days of culture, α-synuclein oligomers could not be detected in axons in the myenteric plexus, circular muscle plexus or tertiary plexus in 4 out of 4 preparations cultured in any of the four conditions (Figures 7-10) using the Syn-O1 antiserum. In addition, labeling of oligomers was not detected in any myenteric nerve cell bodies under any of the conditions tested (Figures 3-10).

Autofluorescent cell bodies in the myenteric plexus during organotypic culture

Faintly autofluorescent nerve cell bodies could be detected in some preparations that had been maintained in organ culture, but not in fresh-fixed preparations. They were visible in all filter sets (Cy3, Cy5, FITC and AMCA), but most readily identified in the FITC filter set (Figure

11). In unlabeled preparations, cultured under the four different conditions for 1-4 days, a blinded observer randomly selected 20 myenteric ganglia and quantified autofluorescent cell bodies. The highest number was counted in tissue exposed to 10μM rotenone after 4 days of culture (Table 5), with similar proportions identified in specimens cultured for 2 and 4 days with 1μM rotenone (Table 5). Autofluorescent cell bodies were clustered in ganglia, with some ganglia containing none, and others containing 10 or more. Autofluorescent cell bodies were too infrequent to count accurately in preparations cultured in standard DME/F12 medium or in medium containing 10mM KCl (see Table 5), but small numbers were present when actively sought out, which could be targeted for subsequent immunohistochemical labeling – see below (Table 6).

Neurochemical coding of autofluorescent cell bodies after organotypic culture

In the present study, preparations labeled with antisera against NOS and ChAT were subsequently visualised with secondary antibodies conjugated to Cy3 and Cy5, respectively. As described in the methods section, autofluorescent nerve cell bodies were clearly visible in using FITC filters (Figure 11) and in unstained preparations in Cy3 and Cy5 filters. However, the autofluorescent signal did not appear to break through into Cy3 and Cy5 channels after NOS and ChAT immunolabeling, presumably because the dim autofluorescent signal was overwhelmed by the background NOS or ChAT immunofluorescence. This allowed us to identify whether autofluorescent nerve cell bodies were immunoreactive for ChAT and/or NOS (Table 6). In all preparations analysed, autofluorescent cell bodies were either ChAT+/NOS- or ChAT-/NOS- (Table 6). ChAT+/NOS- cells were more abundant than ChAT-/NOS- cells (P = 0.0472, Table 6). We also compared the proportions of ChAT+/NOS- and ChAT-/NOS- cell bodies after organ culture after 1-4 days in the four

different solutions (Table 7). In the tissue cultured with 1μM or 10μM rotenone (Figures 12 and 13), after 1, 2 or 4 days of culture the majority of autofluorescent cell bodies were ChAT+/NOS-, with a small proportion being ChAT-/NOS- (Table 7). No NOS-IR neurons were autofluorescent.

DISCUSSION

α-Synuclein is a neuronal protein localized to presynaptic terminals that normally exists as an unfolded, aggregation-prone, monomer or as a stable, aggregation-resistant, tetramer with a rich α-helix conformation (34). These tetramers differ from the pathological oligomers that serve as intermediates to the α-synuclein fibrils that are the major component of Lewy pathology, which vary in size and have a β-sheet conformation (35). A variety of α-synuclein species have been identified in Lewy pathology, including truncated fragments those modified by oxidation, nitration, phosphorylation and ubiquitylation, and those having undergone various stages of aggregation (36). Thus, there may be multiple intermediates in the formation of mature synuclein fibrils. Conventional α-synuclein antibodies do not distinguish α-synuclein species; therefore, conformation-specific antibodies are required to detect specific pathological features of Parkinson's disease.

In this study, we used three α-synuclein antisera to detect changes in α-synuclein expression in enteric neurons following rotenone exposure or raised KCl concentration in ex vivo segments of guinea-pig ileum. Our conventional α-synuclein antibody that detects monomers, oligomers and fibrils did not detect any morphological abnormalities in α-synuclein form or distribution caused by rotenone or KCl. In contrast, the conformation-specific Syn-F2 showed increased expression of α-synuclein fibrils in axons of enteric neurons after rotenone and KCl

treatment. Rotenone also increased the number of autofluorescent cell bodies in myenteric ganglia. The majority of these was immunoreactive for choline acetyltransferase: none was immunoreactive for nitric oxide synthase. This suggests that nitrergic enteric neurons may be selectively less sensitive to rotenone exposure than cholinergic neurons. Notably, nitrergic enteric neurons do not express α-synuclein, whereas nearly all cholinergic neurons do (1). The effects of KCl may be mediated by increased neural excitability and we speculate that this may increase expression of α-synuclein fibrils, although the mechanism is far from clear.

Accumulation of α-synuclein in enteric neurons after organotypic culture

Pathological α-synuclein species have recently been reported in the gastrointestinal tract of patients with Parkinson's disease, but not in age-matched healthy controls (37, 38). However, "pathological" α-synuclein species have been detected in the gut of healthy asymptomatic ageing adults (39, 40, 41, 42). Early studies of the GI tract in Parkinson's disease reported Lewy bodies and neurites comparable to those observed in brain (43, 44, 45). Animal studies have reported morphological changes in α-synuclein localisation in the enteric nervous system of mice expressing *SNCA* mutants associated with Parkinson's disease (46, 47, 48), and after exposure to rotenone (49, 50), and MPTP (51). In this study, we observed an increase in presence of abnormally large axonal varicosities containing α-synuclein, after one or more days in organ culture, with or without raised KCl or rotenone. Whether these swollen varicosities were a consequence of α-synuclein accumulation in terminals, decreased clearance, or accumulation of pathological species is not clear. They were unlikely to be axotomy-induced degeneration, since they were not identified in a previous ultrastructural comparison of fresh and cultured tissue (52). Effects of rotenone on the enteric nervous system may depend on species and region of gut, concentration and exposure to rotenone and

recovery time. Thus, Greene et al., 2009 noted no change in α-synuclein expression in the ileum and proximal colon (53), but an increase was seen in the jejunum (49), duodenum and ileum (54). Another study reported an initial decrease, followed at 6 months by an increase in α-synuclein (50). The present study used concentrations of rotenone and durations of exposure reported to cause α-synuclein accumulation and nerve cell death in brain slices (55, 56), albeit higher than required to cause the first signs of nigrostriatal degeneration (57).

Rotenone and raised KCl concentration cause accumulation of α-synuclein fibrils

α-Synuclein fibrils are the major component of Lewy bodies and neurites (2, 3, 4). *SNCA* missense mutations underlie some cases of Parkinson's disease and accelerate formation of α-synuclein oligomers and fibrils (58, 59), which are toxic (60, 61), causing synaptic and nerve cell degeneration, and seeding aggregation of endogenous α-synuclein in central and peripheral nerve cells (20, 21). Here, we observed accumulation of α-synuclein fibrils in the axons, but not cell bodies, of cholinergic interneurons and motorneurons in the guinea-pig ileum after exposure to rotenone in a concentration- and time-dependent manner. Raising KCl concentration in medium for 1-4 days also caused accumulation of α-synuclein fibrils in these same axons, but not cell bodies.

This occurred despite no detectable overall morphological changes in α-synuclein detected by conventional antiserum. No accumulation of α-synuclein oligomers was detected with a conformation-specific antiserum under the same conditions. The Syn-F2 and Syn-O1 antibodies do not recognize the same epitopes (30). The Syn-F2 antibody preferentially binds more mature synuclein fibrils, whilst Syn-O1 antibody recognizes both early α-synuclein oligomers as well as late synuclein fibrils (30).

The mechanisms of how raised [K+] and rotenone cause fibril formation were not investigated. However, production of α-synuclein fibrils may be related to its role in the synaptic vesicle cycle. Neurotransmitter release requires assembly of SNARE complexes that facilitate fusion pore formation (62). SNARE complex assembly and disassembly occurs repeatedly during periods of fast action potential firing, often at considerable distances from the nerve cell body. SNARE proteins form highly reactive intermediates that can misfold and aggregate (63, 64). α-Synuclein appears to function as a molecular chaperone of the v-SNARE, synaptobrevin-2, limiting its misfolding and aggregation (63). It may become a victim of bystander damage inflicted by such reactive intermediates, leading to dissociation of the stable tetrameric form (65) intro unstable monomers. If protective mechanisms are overwhelmed during periods of prolonged high frequency firing, perhaps due to ATP depletion driven by demands of the Na+/K+ ATPase, this could explain the effects of raised [K+] in vitro on fibril formation.

Rotenone causes necrosis of cholinergic enteric neurons

Exposure to rotenone evoked autofluorescence in many nerve cell bodies, consistent with ongoing necrosis (66, 67, 68, 69). Over 80% of these cell bodies were immunoreactive for the cholinergic marker, ChAT. The remainder lacked both ChAT and NOS immunoreactivity. Cholinergic neurons comprise from 68-81% of myenteric neurons in guinea pig small intestine (70; 71) and α-synuclein is restricted to cholinergic neurons in this same preparation (1). What is most striking about these figures is that none of the autofluorescent cells was immunoreactive for nitric oxide synthase, despite NOS being present in 20-25% of myenteric neurons in guinea pig ileum (72). This either suggests that NOS-containing neurons are resistant to rotenone-induced necrosis, or that NOS immunoreactivity is lost from necrotic

nerve cells. If rotenone's toxicity is mediated through aggregation of α-synuclein, then this may explain the selective loss of cholinergic neurons in our preparation, as nitrergic neurons do not express α-synuclein (1, 32). Nitric oxide synthase may have a neuroprotective effect on enteric neurons in inflammation (73) and ischemia/reperfusion (74). Reactive oxygen species are produced in ischemia/reperfusion (75); it is possible that NOS-containing neurons have higher levels of endogenous antioxidants to cope with reactive oxygen species during nitric oxide synthesis.

α-Synuclein as a biomarker and therapeutic target in the GI tract

Using a threshold dilution, we achieved selective immunolabeling for α-synuclein fibrils in the enteric nervous system. Potentially, this may be a simple way of determining whether pathological α-synuclein species are elevated in Parkinson's disease. α-Synuclein accumulates in the gut in the preclinical stage of Parkinson's disease, it is possible that conformation-specific antibodies to α-synuclein fibrils may be useful in early diagnosis based on colonic biopsies.

In conclusion, rotenone exposure and prolonged raised [K+] caused accumulation of α-synuclein fibrils in the axons of cholinergic enteric neurons. This took place in a time- and, in the case of rotenone, concentration-dependent manner. Rotenone also caused selective necrosis of cholinergic enteric neurons in a concentration-dependent manner. Conformation-specific antibodies to α-synuclein may be valuable tools for assessment of pathological features in the enteric nervous system.

AUTHOR CONTRIBUTIONS

DFS designed the study, performed the research, analysed data, and wrote the manuscript; BNC performed the research; NV and OME provided essential reagents; WP and SJH designed the study and wrote the manuscript.

LITERATURE CITED

1. Sharrad DF, de Vries E, Brookes SJ. 2013a. Selective expression of α-synuclein-immunoreactivity in vesicular acetylcholine transporter-immunoreactive axons in the guinea pig rectum and human colon. J Comp Neurol. 521(3):657-76.

2. Spillantini MG, Schmidt ML, Lee VM, Trojanowski JQ, Jakes R, Goedert M. 1997. Alpha-synuclein in Lewy bodies. Nature. 388(6645):839-40.

3. Irizarry MC, Growdon W, Gomez-Isla T, Newell K, George JM, Clayton DF, Hyman BT. 1998. Nigral and cortical Lewy bodies and dystrophic nigral neurites in Parkinson's disease and cortical Lewy body disease contain alpha-synuclein immunoreactivity. J Neuropathol Exp Neurol. 57(4):334-7.

4. Baba M, Nakajo S, Tu PH, Tomita T, Nakaya K, Lee VM, Trojanowski JQ, Iwatsubo T. 1998. Aggregation of alpha-synuclein in Lewy bodies of sporadic Parkinson's disease and dementia with Lewy bodies. Am J Pathol. 152(4):879-84.

5. Hawkes CH, Del Tredici K, Braak H. 2010. A timeline for Parkinson's disease. Parkinsonism Relat Disord. 16(2):79-84.

6. Braak H, Del Tredici K, Rüb U, de Vos RA, Jansen Steur EN, Braak E. 2003. Staging of brain pathology related to sporadic Parkinson's disease. Neurobiol Aging. 24(2):197-211.

7. Braak H, de Vos RA, Bohl J, Del Tredici K. 2006. Gastric alpha-synuclein immunoreactive inclusions in Meissner's and Auerbach's plexuses in cases staged for Parkinson's disease-related brain pathology. Neurosci Lett. 396(1):67-72.

8. Del Tredici K, Braak H. 2015. Sporadic Parkinson's disease: development and distribution of α-synuclein pathology. Neuropathol Appl Neurobiol. doi: 10.1111/nan.12298.

9. Hely MA, Morris JG, Reid WG, Trafficante R. 2005. Sydney Multicenter Study of Parkinson's disease: non-L-dopa-responsive problems dominate at 15 years. Mov Disord. vol. 20, pp. 190-199.

10. Gulati A, Forbes A, Stegie F, Kelly L, Clough C, Chaudhuri KR. 2004. A clinical observational study of the pattern and occurrence of non-motor symptoms in Parkinson’s disease ranging from early to advanced disease. Mov Disord. vol. 19 (Suppl 9), pp. S406.

11. Chaudhuri KR, Yates L, Martinez-Martin P. 2005. The non-motor symptom complex of Parkinson's disease: a comprehensive assessment is essential. Curr Neurol Neurosci Rep. 5(4):275-83.

12. Pagano G, Tan EE, Haider JM, Bautista A, Tagliati M. 2015. Constipation is reduced by beta-blockers and increased by dopaminergic medications in Parkinson's disease. Parkinsonism Relat Disord. 2015 Feb;21(2):120-5.

13. Wakabayashi K, Takahashi H. 1997a. Neuropathology of autonomic nervous system in Parkinson's disease. Eur Neurol. 38 Suppl 2:2-7.

14. Fasano A, Visanji NP, Liu LW, Lang AE, Pfeiffer RF. 2015. Gastrointestinal dysfunction in Parkinson's disease. Lancet Neurol. 14(6):625-39.

15. Adams-Carr KL, Bestwick JP, Shribman S, Lees A, Schrag A, Noyce AJ. 2015. Constipation preceding Parkinson's disease: a systematic review and meta-analysis. J Neurol Neurosurg Psychiatry. 2015 Sep 7. pii: jnnp-2015-311680. doi: 10.1136/jnnp-2015-311680. [Epub ahead of print]

16. Hilton D, Stephens M, Kirk L, Edwards P, Potter R, Zajicek J, Broughton E, Hagan H, Carroll C. 2014. Accumulation of α-synuclein in the bowel of patients in the pre-clinical phase of Parkinson's disease. Acta Neuropathol. 127(2):235-41.

17. Hernandez DG, Reed X, Singleton AB. 2016. Genetics in Parkinson disease: Mendelian versus non-Mendelian inheritance. J Neurochem. doi: 10.1111/jnc.13593. [Epub ahead of print]

18. Tokuda, T, Qureshi, M.M., Ardah, M.T., Varghese, S., Shehab, S.A., Kasai, T., Ishigami, N.,

Tamaoka, A., Nakagawa, M., El-Agnaf, O.M., 2010. Detection of elevated levels of α-synuclein oligomers in CSF from patients with Parkinson disease. Neurology 75, 1766–1772

19. Hansson, O., Hall, S., Ohrfelt, A., Zetterberg, H., Blennow, K., Minthon, L., Nagga, K., Londos,E., Varghese, S., Majbour, N.K., Al-Hayani, A., El-Agnaf, O.M., 2014. Levels of cerebrospinal fluid alpha-synuclein oligomers are increased in Parkinson's disease with dementia and dementia with Lewy bodies compared to Alzheimer's disease. Alzheimers Res. Ther. 6, 25.

20. Luk, K.C., Kehm, V., Carroll, J., Zhang, B., O'Brien, P., Trojanowski, J.Q., Lee, V.M., 2012. Pathological alpha-synuclein transmission initiates Parkinson-like neurodegeneration in nontransgenic mice. Science. 338, 949–953.

21. Sacino, A.N., Brooks, M., Thomas, M.A., McKinney, A.B., Lee, S., Regenhardt, R.W., McGarvey, N.H., Ayers, J.I., Notterpek, L., Borchelt, D.R., Golde, T.E., Giasson, B.I., 2014. Intramuscular injection of alpha-synuclein induces CNS alpha-synuclein pathology and a rapid-onset motor phenotype in transgenic mice. Proc. Natl. Acad. Sci. USA. 111, 10732–10737.

22. Holmqvist S, Chutna O, Bousset L, Aldrin-Kirk P, Li W, Björklund T, Wang ZY, Roybon L, Melki R, Li JY. 2014. Direct evidence of Parkinson pathology spread from the gastrointestinal tract to the brain in rats. Acta Neuropathol. 128(6):805-20.

23. Moon HE, Paek SH. 2015. Mitochondrial Dysfunction in Parkinson's Disease. Exp Neurobiol. 24(2):103-16.

24. Lai BC, Marion SA, Teschke K, Tsui JK. 2002. Occupational and environmental risk factors for Parkinson's disease. Parkinsonism Relat Disord. 8(5):297-309.

25. Schapira AH, Cooper JM, Dexter D, Jenner P, Clark JB, Marsden CD. 1989. Mitochondrial complex I deficiency in Parkinson's disease. Lancet. 1(8649):1269.

26. Betarbet R, Sherer TB, MacKenzie G, Garcia-Osuna M, Panov AV, Greenamyre JT. 2000. Chronic systemic pesticide exposure reproduces features of Parkinson's disease. Nat Neurosci. 3(12):1301-6.

27. Sherer TB, Betarbet R, Stout AK, Lund S, Baptista M, Panov AV, Cookson MR, Greenamyre JT. 2002. An in vitro model of Parkinson's disease: linking mitochondrial impairment to altered alpha-synuclein metabolism and oxidative damage. J Neurosci. 22(16):7006-15.

28. Follett J, Darlow B, Wong MB, Goodwin J, Pountney DL. Potassium depolarization and raised calcium induces α-synuclein aggregates. Neurotox Res. 2013 May;23(4):378-92

29. Surmeier DJ, Guzman JN, Sanchez J, Schumacker PT. 2012. Physiological phenotype and vulnerability in Parkinson's disease. Cold Spring Harb Perspect Med.2(7):a009290.

30. Vaikath NN, Majbour NK, Paleologou KE, Ardah MT, van Dam E, van de Berg WD, Forrest SL, Parkkinen L, Gai WP, Hattori N, Takanashi M, Lee SJ, Mann DM, Imai Y, Halliday GM, Li JY, El-Agnaf OM. 2015. Generation and characterization of novel

conformation-specific monoclonal antibodies for α-synuclein pathology. Neurobiol Dis. 79:81-99.

31. Birder LA, Kanai AJ, de Groat WC. DMSO: effect on bladder afferent neurons and nitric oxide release. J Urol. 1997 Nov;158(5):1989-95.

32. Gai WP, Power JH, Blumbergs PC, Culvenor JG, Jensen PH. 1999. Alpha-synuclein immunoisolation of glial inclusions from multiple system atrophy brain tissue reveals multiprotein components. J Neurochem. 73(5):2093-100.

33. Sharrad DF, Gai WP, Brookes SJ. 2013b. Selective coexpression of synaptic proteins, α-synuclein, cysteine string protein-α, synaptophysin, synaptotagmin-1, and synaptobrevin-2 in vesicular acetylcholine transporter-immunoreactive axons in the guinea pig ileum. J Comp Neurol. 521(11):2523-37.

34. Dettmer U, Selkoe D, Bartels T. 2016. New insights into cellular α-synuclein homeostasis in health and disease. Curr Opin Neurobiol. 36:15-22.

35. Wang W, Perovic I, Chittuluru J, Kaganovich A, Nguyen LT, Liao J, Auclair JR, Johnson D, Landeru A, Simorellis AK, Ju S, Cookson MR, Asturias FJ, Agar JN, Webb BN, Kang C, Ringe D, Petsko GA, Pochapsky TC, Hoang QQ. 2011. A soluble a-synuclein construct forms a dynamic tetramer. Proc Natl Acad Sci USA. 108:17797-17802.

36. Peelaerts W, Baekelandt V. 2016. α-Synuclein strains and the variable pathologies of synucleinopathies. J Neurochem. doi: 10.1111/jnc.13595. [Epub ahead of print]

37. Lebouvier T, Chaumette T, Damier P, Coron E, Touchefeu Y, Vrignaud S, Naveilhan P, Galmiche JP, Bruley des Varannes S, Derkinderen P, Neunlist M. 2008. Pathological lesions in colonic biopsies during Parkinson's disease. Gut. 57(12):1741-3.

38. Pouclet H, Lebouvier T, Coron E, Des Varannes SB, Neunlist M, Derkinderen P. 2012. A comparison between colonic submucosa and mucosa to detect Lewy pathology in Parkinson's disease. Neurogastroenterol Motil. 24(4):e202-5.

39. Böttner M, Zorenkov D, Hellwig I, Barrenschee M, Harde J, Fricke T, Deuschl G, Egberts JH, Becker T, Fritscher-Ravens A, Arlt A, Wedel, T. 2012. Expression pattern and localization of alpha-synuclein in the human enteric nervous system, Neurobiol. Dis. 48(3):474–480.

40. N.P. Visanji, C. Marras, D.S. Kern, A. Al Dakheel, A. Gao, L.W. Liu, A.E. Lang, L.N. Hazrati. 2015. Colonic mucosal a-synuclein lacks specificity as a biomarker for Parkinson disease. Neurology. 84(6):609–616

41. Chung SJ, Kim J, Lee HJ, Ryu HS, Kim K, Lee JH, Jung KW, Kim MJ, Kim MJ, Kim YJ, Yun SC, Lee JY, Hong SM, Myung SJ. 2015. Alpha-synuclein in gastric and colonic mucosa in Parkinson's disease: Limited role as a biomarker. Mov Disord. doi: 10.1002/mds.26473. [Epub ahead of print]

42. Aldecoa I, Navarro-Otano J, Stefanova N, Sprenger FS, Seppi K, Poewe W, Cuatrecasas M, Valldeoriola F, Gelpi E, Tolosa E. 2015. Alpha-synuclein immunoreactivity patterns in the enteric nervous system. Neurosci Lett. 602:145-9.

43. Qualman SJ, Haupt HM, Yang P, Hamilton SR. 1984. Esophageal Lewy bodies associated with ganglion cell loss in achalasia. Similarity to Parkinson's disease. Gastroenterology. 87:848–856.

44. Kupsky WJ, Grimes MM, Sweeting J, Bertsch R, Cote LJ. 1987. Parkinson's disease and megacolon: concentric hyaline inclusions (Lewy bodies) in enteric ganglion cells. Neurology. 37:1253–1255.

45. Wakabayashi K, Takahashi H, Takeda S, Ohama E, Ikuta F. 1988. Parkinson's disease: the presence of Lewy bodies in Auerbach's and Meissner's plexuses. Acta Neuropathol. 1988;76(3):217-221.

46. Wang L, Magen I, Yuan PQ, Subramaniam SR, Richter F, Chesselet MF, Taché Y. 2012. Mice overexpressing wild-type human alpha-synuclein display alterations in colonic myenteric ganglia and defecation. Neurogastroenterol Motil. 24(9):e425-36.

47. Hallett PJ, McLean JR, Kartunen A, Langston JW, Isacson O. 2012. α-Synuclein overexpressing transgenic mice show internal organ pathology and autonomic deficits. Neurobiol Dis. 47(2):258-67.

48. Kuo YM, Li Z, Jiao Y, Gaborit N, Pani AK, Orrison BM, Bruneau BG, Giasson BI, Smeyne RJ, Gershon MD, Nussbaum RL. 2010. Extensive enteric nervous system abnormalities in mice transgenic for artificial chromosomes containing Parkinson disease-associated alpha-synuclein gene mutations precede central nervous system changes. Hum Mol Genet. 19(9):1633-50.

49. Tasselli M, Chaumette T, Paillusson S, Monnet Y, Lafoux A, Huchet-Cadiou C, Aubert P, Hunot S, Derkinderen P, Neunlist M. 2013. Effects of oral administration of rotenone on gastrointestinal functions in mice. Neurogastroenterol Motil. 25(3):e183-93.

50. Drolet RE, Cannon JR, Montero L, Greenamyre JT. 2009. Chronic rotenone exposure reproduces Parkinson's disease gastrointestinal neuropathology. Neurobiol Dis. 36(1):96-102.

51. Natale G, Kastsiushenka O, Fulceri F, Ruggieri S, Paparelli A, Fornai F. 2010. MPTP-induced parkinsonism extends to a subclass of TH-positive neurons in the gut. Brain Res. 1355:195-206.

52. Song ZM, Brookes SJ, Llewellyn-Smith IJ, Costa M. 1995. Ultrastructural studies of the myenteric plexus and smooth muscle in organotypic cultures of the guinea-pig small intestine. Cell Tissue Res. 280(3):627-37.

53. Greene JG, Noorian AR, Srinivasan S. 2009. Delayed gastric emptying and enteric nervous system dysfunction in the rotenone model of Parkinson's disease. Exp Neurol. 218(1):154-61.

54. Pan-Montojo F, Anichtchik O, Dening Y, Knels L, Pursche S, Jung R, Jackson S, Gille G, Spillantini MG, Reichmann H, Funk RH. 2010. Progression of Parkinson's disease pathology is reproduced by intragastric administration of rotenone in mice. PLoS One. 5(1):e8762.

55. Moldzio R, Piskernik C, Radad K, Rausch WD. 2008. Rotenone damages striatal organotypic slice culture. Ann N Y Acad Sci. 1148:530-5.

56. Ullrich C, Humpel C. 2009. Rotenone induces cell death of cholinergic neurons in an organotypic co-culture brain slice model. Neurochem Res. 34(12):2147-53.

57. Testa CM, Sherer TB, Greenamyre JT. 2005. Rotenone induces oxidative stress and dopaminergic neuron damage in organotypic substantia nigra cultures. Brain Res Mol Brain Res. 134(1):109-18.

58. Narhi L, Wood SJ, Steavenson S, Jiang Y, Wu GM, Anafi D, Kaufman SA, Martin F, Sitney K, Denis P, Louis JC, Wypych J, Biere AL, Citron M. 1999. Both familial Parkinson's disease mutations accelerate alpha-synuclein aggregation. J Biol Chem. 274(14):9843-6.

59. Conway KA, Lee SJ, Rochet JC, Ding TT, Williamson RE, Lansbury PT Jr. 2000. Acceleration of oligomerization, not fibrillization, is a shared property of both alpha-synuclein mutations linked to early-onset Parkinson's disease: implications for pathogenesis and therapy. Proc Natl Acad Sci USA. 97(2):571-6.

60. Rockenstein, E., Nuber, S., Overk, C.R., Ubhi, K., Mante, M., Patrick, C., Adame, A., TrejoMorales, M., Gerez, J., Picotti, P., Jensen, P.H., Campioni, S., Riek, R., Winkler, J., Gage, F.H., Winner, B., Masliah, E. 2014. Accumulation of oligomer-prone alpha-synuclein exacerbates synaptic and neuronal degeneration in vivo. Brain. 137, 1496–1513.

61. Winner, B., Jappelli, R., Maji, S.K., Desplats, P.A., Boyer, L., Aigner, S., Hetzer, C., Loher, T., Vilar, M., Campioni, S., Tzitzilonis, C., Soragni, A., Jessberger, S., Mira, H., Consiglio, A., Pham, E., Masliah, E., Gage, F.H., Riek, R., 2011. In vivo demonstration that alphasynuclein oligomers are toxic. Proc. Natl. Acad. Sci. USA. 108, 4194–4199.

62. Jahn R, Scheller RH. 2006. SNAREs--engines for membrane fusion. Nat Rev Mol Cell Biol. 7(9):631-43.

63. Burré J, Sharma M, Tsetsenis T, Buchman V, Etherton MR, Südhof TC. 2010. Alpha-synuclein promotes SNARE-complex assembly in vivo and in vitro. Science. 329(5999):1663-7.

64. Sharma M, Burré J, Südhof TC. 2011. CSPα promotes SNARE-complex assembly by chaperoning SNAP-25 during synaptic activity. Nat Cell Biol. 13(1):30-9.

65. Burré J, Sharma M, Südhof TC. 2014. α-Synuclein assembles into higher-order multimers upon membrane binding to promote SNARE complex formation. Proc Natl Acad Sci USA. 111(40):E4274-83.

66. Allwork SP, Bentall HH. 1986. Usefulness of the phenomenon of histofluorescence in the identification of early myocardial necrosis. Cardiovasc Res. 20:451–457.

67. Salinas-Madrigal L, Sotelo-Avila C. 1986. Morphologic diagnosis of acute tubular necrosis (ATN) by autofluorescence. Am J Kidney Dis. 7:84–87.

68. Chopra P, Sabherwal U. Histochemical and fluorescent techniques for detection of early myocardial ischemia following experimental coronary artery occlusion: A comparative and quantitative study.Angiology. 1988;39:132–140.

69. Anderson CD, Lin WC, Beckham J, Mahadevan-Jansen A, Buttemere CR, Pierce J, Nicoud IB, Wright Pinson C, Chari RS. 2004. Fluorescence spectroscopy accurately detects irreversible cell damage during hepatic radiofrequency ablation. Surgery. 136:524–531.

70. Steele PA, Brookes SJ, Costa M. 1991. Immunohistochemical identification of cholinergic neurons in the myenteric plexus of guinea-pig small intestine. Neuroscience. 45(1):227-39.

71. Costa M, Furness JB, Pompolo S, Brookes SJ, Bornstein JC, Bredt DS, Snyder SH. 1992. Projections and chemical coding of neurons with immunoreactivity for nitric oxide synthase in the guinea-pig small intestine. Neurosci Lett. 148(1-2):121-5.

72. Costa M, Brookes SJ, Steele PA, Gibbins I, Burcher E, Kandiah CJ. 1996. Neurochemical classification of myenteric neurons in the guinea-pig ileum. Neuroscience. 75(3):949-67.

73. Miller MJ, Munshi UK, Sadowska-Krowicka H, Kakkis JL, Zhang XJ, Eloby-Childress S, Clark DA. 1994. Inhibition of calcium-dependent nitric oxide synthase causes ileitis and leukocytosis in guinea pigs. Dig Dis Sci. 39(6):1185-92.

74. Rivera LR, Pontell L, Cho HJ, Castelucci P, Thacker M, Poole DP, Frugier T, Furness JB. 2012. Knock out of neuronal nitric oxide synthase exacerbates intestinal ischemia/reperfusion injury in mice. Cell Tissue Res. 349(2):565-76.

75. Kalogeris T, Bao Y, Korthuis RJ. 2014. Mitochondrial reactive oxygen species: a double edged sword in ischemia/reperfusion vs preconditioning. Redox Biol. 2:702-14.

Primary Antibody	Immunising antigen	Manufacturer, catalogue #, lot #	Dilution	Raised
α-Synuclein	Human α -synuclein residue 116-131 (peptide sequence: MPVDPDNEAYEMPSEEC)	Gai et al., (1999)	1:1000	Sheep
Syn-F2	α-synuclein fibrils	Vaikath et al., (2015)	1:200	Mouse
Syn-O1	α-synuclein fibrils	Vaikath et al., (2015)	1:1500	Mouse
ChAT	Peptide fragment of purified porcine ChAT (GLFSSYR LPGHTQDTLVAQKSS) 22 amino acids: 168-189	Schemann/P3YEB	1:500	Rabbit
NOS	Recombinant rat neuronal NOS	Emson/K205	1:1000	Sheep

Table 1. Primary antisera used in the study

Secondary Antibody	Manufacturer and catalogue #	Dilution	Raised	Conjugated fluorophore
Donkey anti-sheep IgG	Jackson, 71 165 147	1:200	Donkey	Cy3
Donkey anti-rabbit IgG	Jackson, 711 175 152	1:200	Donkey	Cy5
Donkey anti-mouse IgG	Jackson, 715 165 151	1:200	Donkey	Cy3

Table 2. Secondary antisera used in the study

	Normal varicosities	Abnormally large varicosities
Mean area ± SEM	$0.21 \pm 0.0\ \mu m^2$	$1.39 \pm 0.1\ \mu m^2$

n=4

Table 3. Mean area of normal and abnormally large a-synuclein varicosities in the tertiary plexus after various conditions of culture of different duration

	Fresh fixed tissue (Mean ± SEM, range)	Standard medium (Mean ± SEM, range)	1µm rotenone (Mean ± SEM, range)	10µm rotenone (Mean ± SEM, range)	10mM KCl (Mean ± SEM, range)

Day 1	0 ± 0 (0-0)	4 ± 4 (0-14)	12 ± 7 (1-28)	5 ± 2 (2-5)	17 ± 9 (2-7)
Day 2	0 ± 0 (0-0)	34 ± 18 (5-39)	47 ± 22 (10-65)	17 ± 6 (7-27)	17 ± 9 (0-37)
Day 4	0 ± 0 (0-0)	18 ± 13 (1-27)	21 ± 14 (4-53)	52 ± 28 (3-87)	17 ± 11 (8-22)

n=4

Table 4. Mean proportion of abnormally large varicosities containing α-synuclein in the tertiary plexus

	Control (Mean ± SEM, range # cells)	**10mM KCl (Mean ± SEM, range # cells)**	**1µm rotenone (Mean ± SEM, range # cells)**	**10µm rotenone (Mean ± SEM, range # cells)**
Day 1	0 ± 0	0 ± 0	0 ± 0	14 ± 8 (0-20)
Day 2	0 ± 0	0 ± 0	34 ± 11 (0-27)	16 ± 15 (0-11)
Day 4	0 ± 0	0 ± 0	33 ± 17 (0-20)	50 ± 29 (3-60)

n=4

Table 5. Mean proportion of autofluorescent cell bodies in the myenteric plexus after the four conditions of culture of 1-4 days duration

	ChAT+/NOS-	**ChAT-/NOS-**
Mean ± SEM, range	74 ± 22 (17-121)	18 ± 3.4 (8-24)

n = 4

Table 6. Mean number of nerve cell bodies that were ChAT+/NOS- or ChAT-/NOS- after pooling all autofluorescent cell bodies sampled after the four conditions of culture of 1-4 days duration

	Control (Mean ± SEM, range # cells)		**10mM KCl (Mean ± SEM, range # cells)**		**1µm rotenone (Mean ± SEM, range # cells)**		**10µm rotenone (Mean ± SEM, range # cells)**	
	ChAT+/ NOS-	ChAT- /NOS-	ChAT+/ NOS-	ChAT- /NOS-	ChAT+/ NOS-	ChAT/N OS-	ChAT+/ NOS-	ChAT- /NOS-
Day 1	6 ± 6 (0-6)	0 ± 0	30 ± 23.9 (0-27)	8 ± 8 (0-9)	27 ± 17 (0-13)	0 ± 0	34 ± 22 (3-27)	13 ± 9 (0-5)
Day 2	8 ± 9 (0-9)	0 ± 0	9 ± 6 (0-6)	15 ± 15 (0-8)	32 ± 13 (0-16)	6 ± 4 (0-4)	47 ± 21 (0-14)	14 ± 9 (0-5)
Day 4	15 ± 7 (0-8)	13 ± 7 (0-7)	14 ± 9 (0-10)	6 ± 4 (0-4)	27 ± 17 (0-19)	11 ± 5 (0-4)	38 ± 23 (0-32)	1 ± 1 (0-1)

n=4

Table 7. Mean proportion of ChAT+/NOS- and ChAT-/NOS- autofluorescent cell bodies in the myenteric plexus after the four conditions of culture of 1-4 days duration

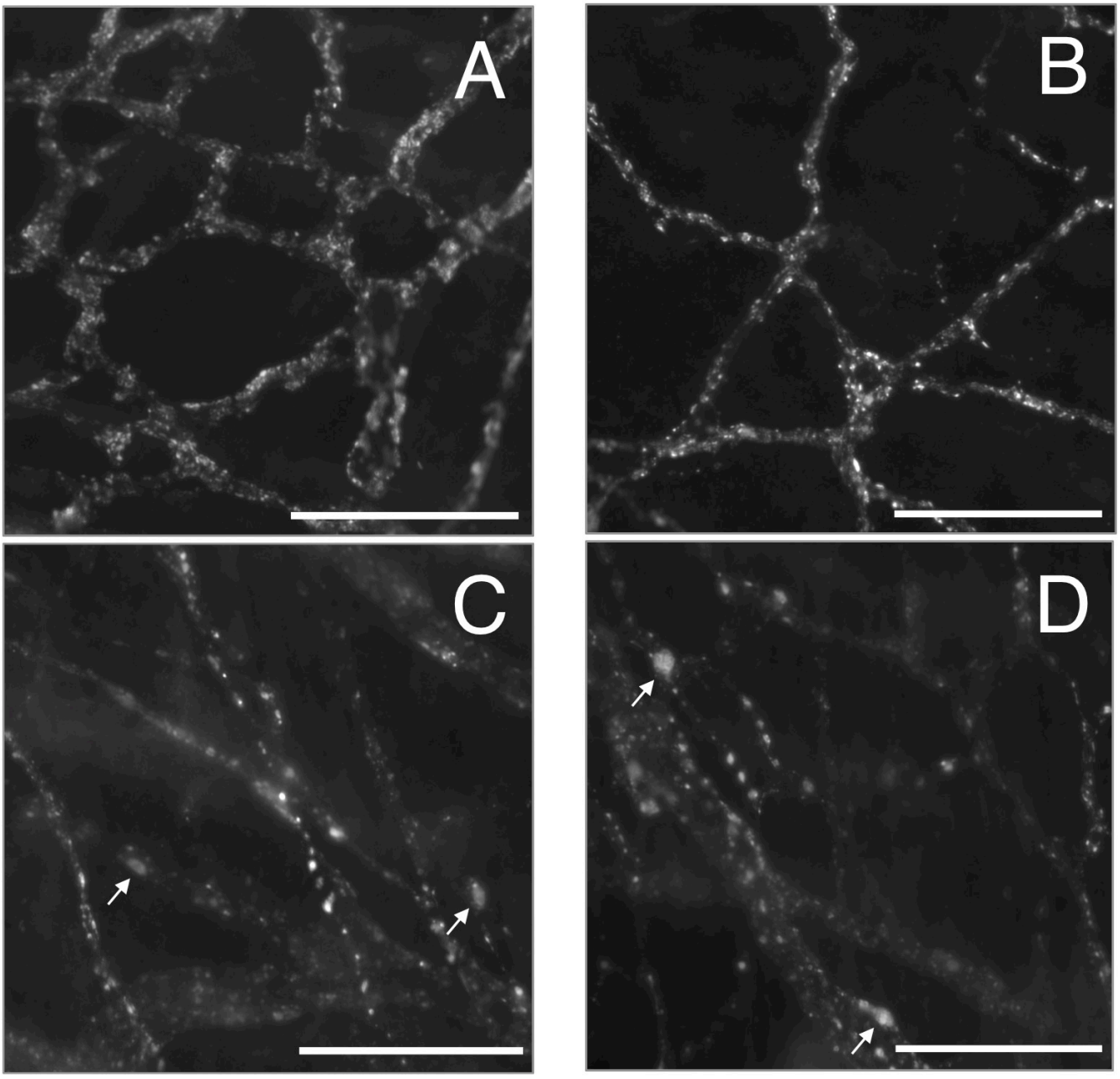
A
B
C
D

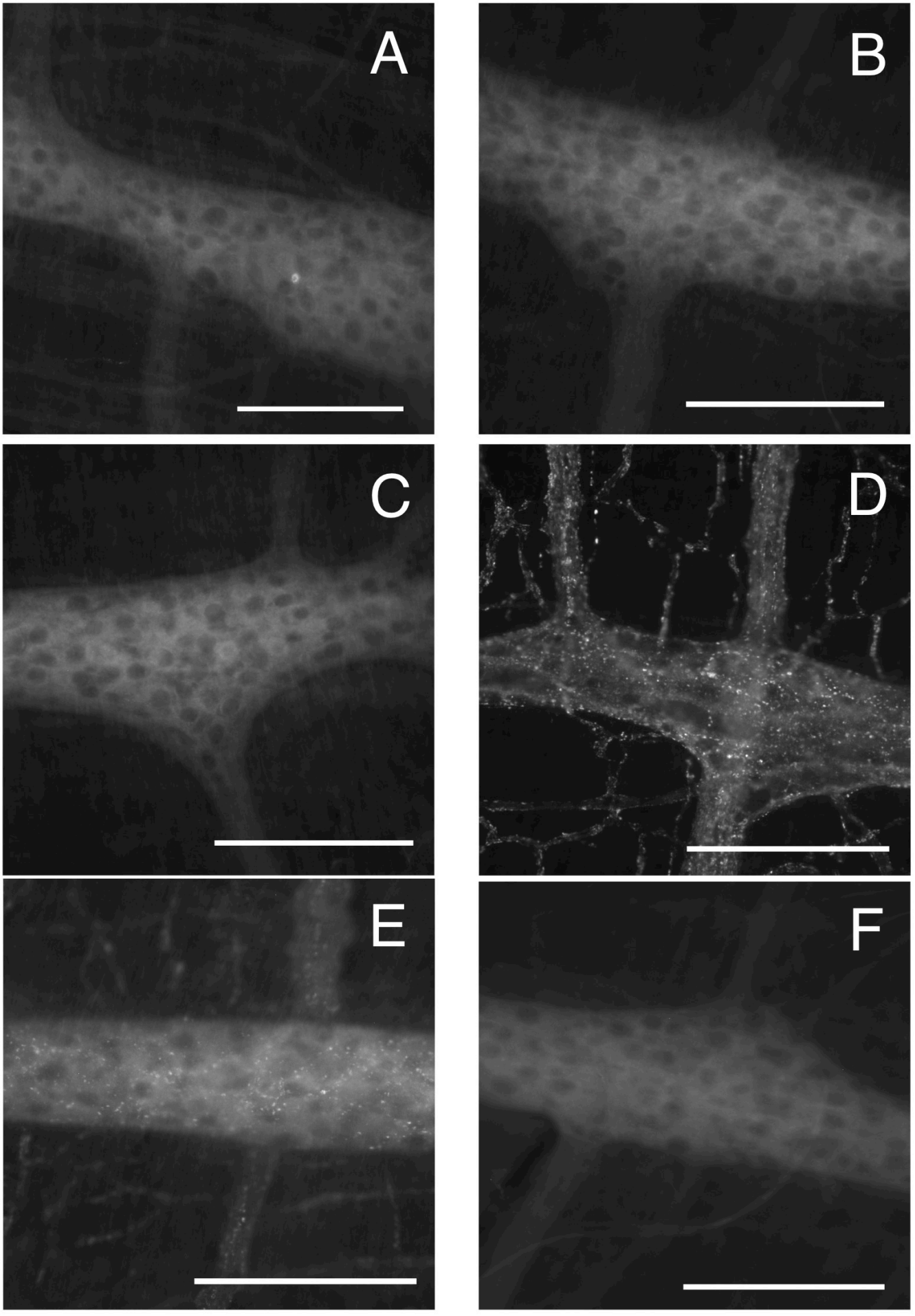
A
B
C
D
E
F

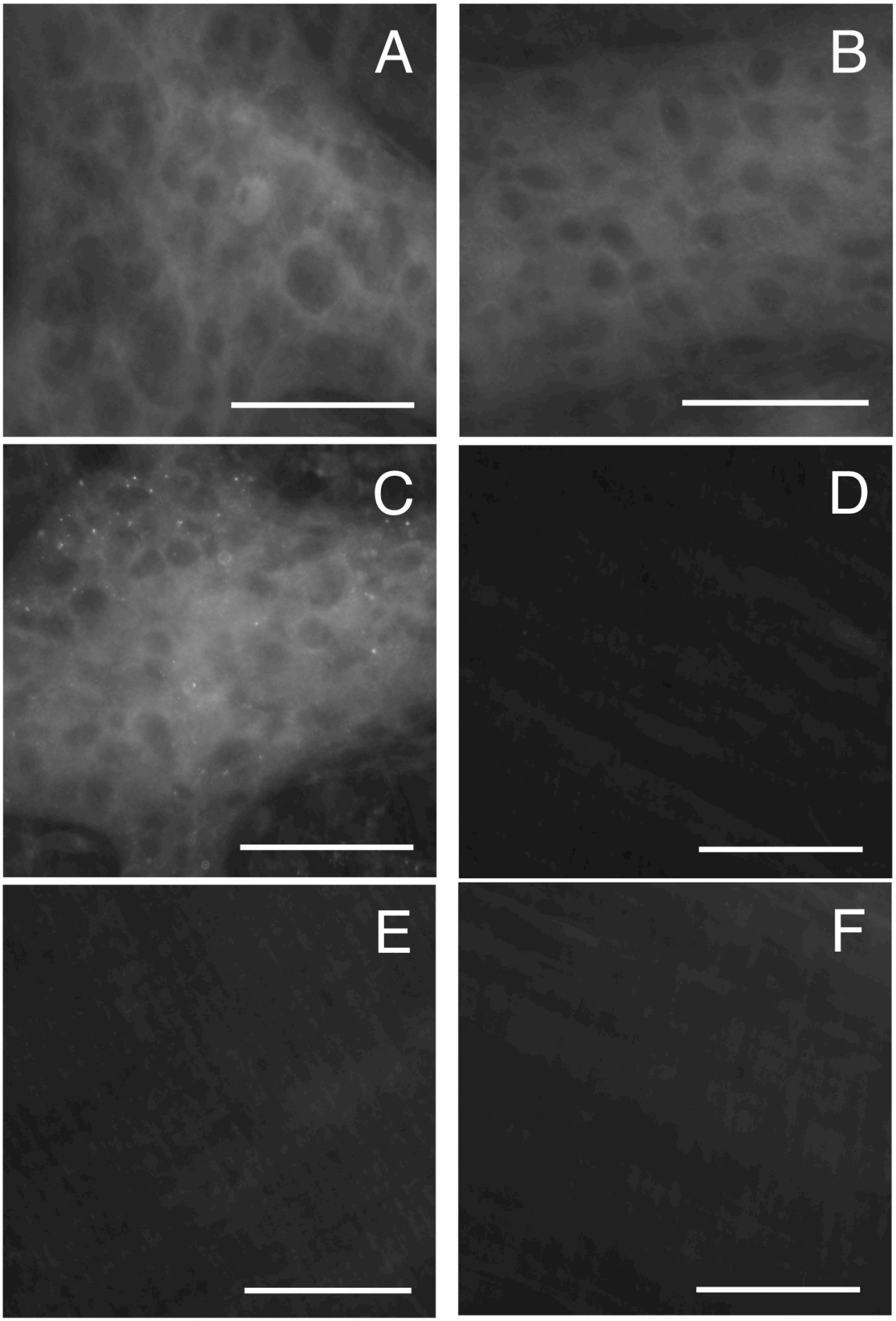
A
B
C
D
E
F

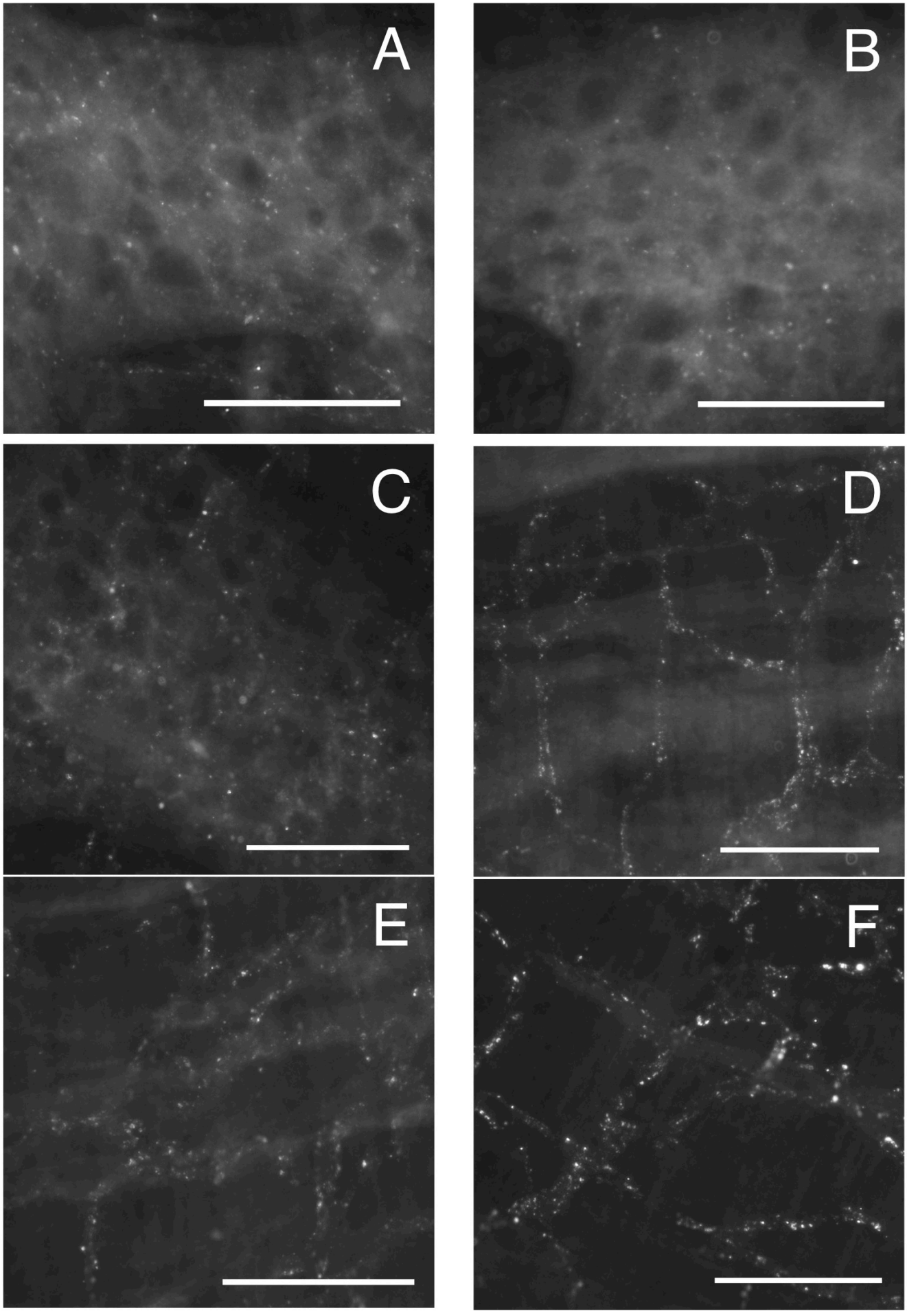
A
B
C
D
E
F

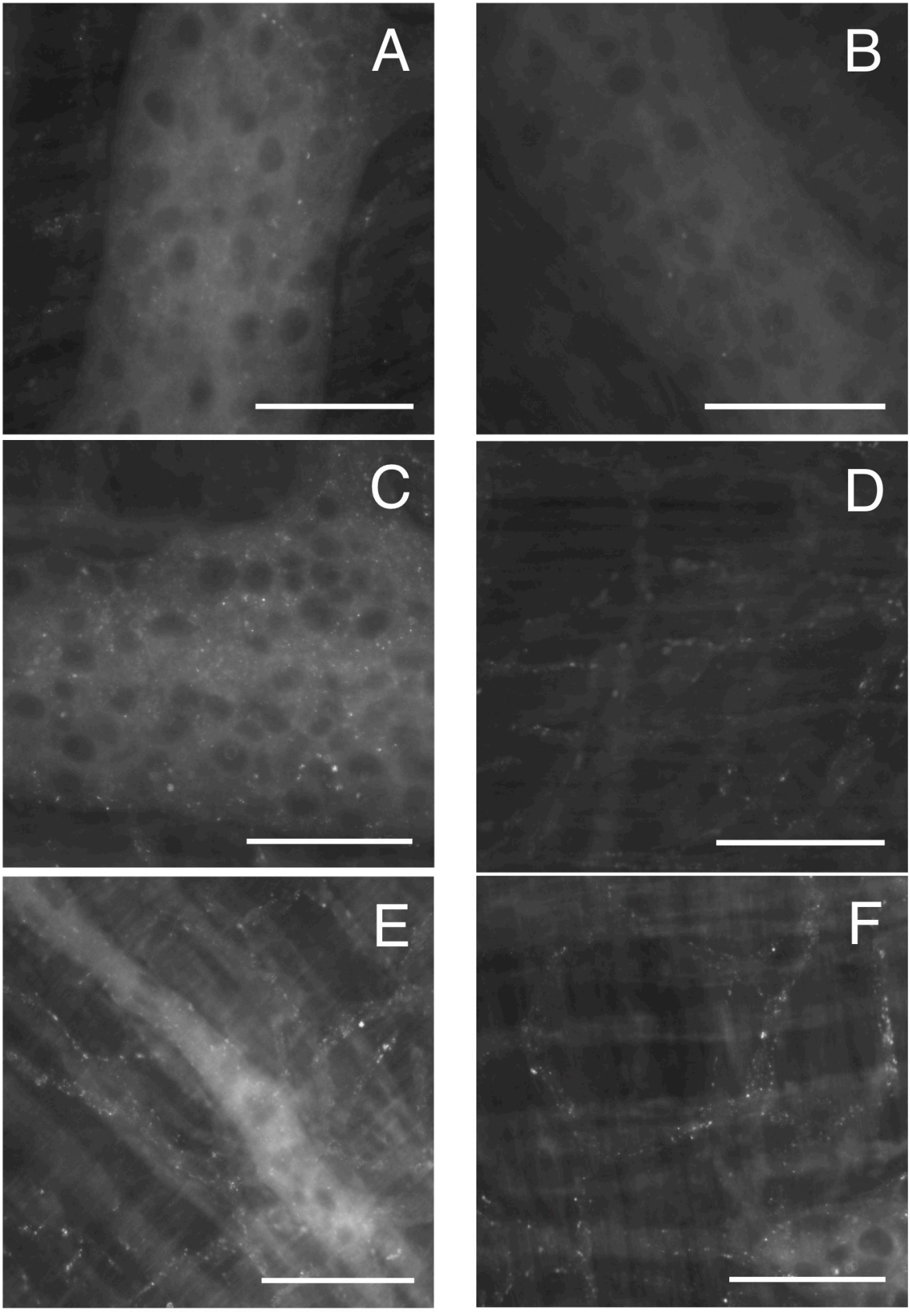
A
B
C
D
E
F

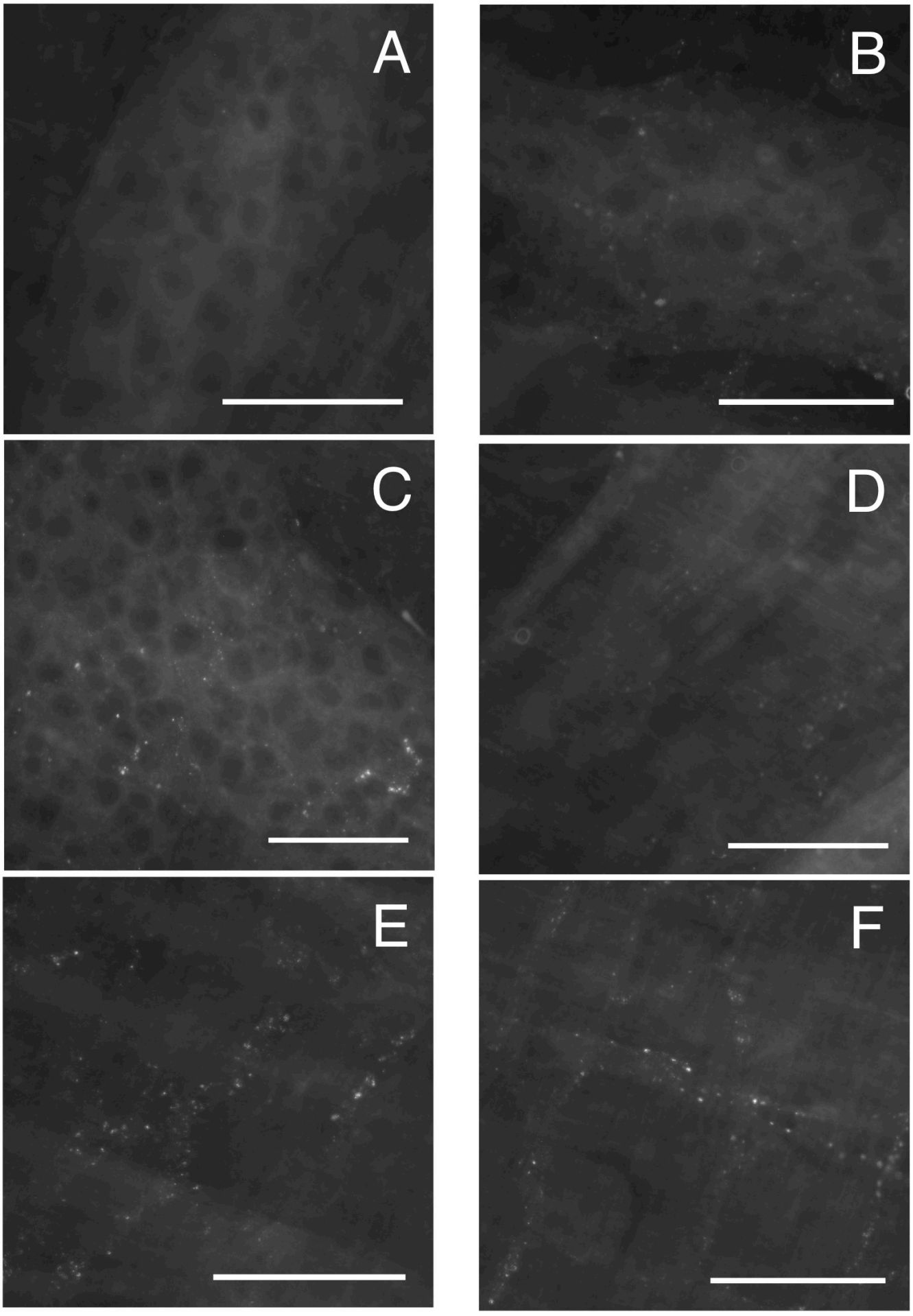
A
B
C
D
E
F

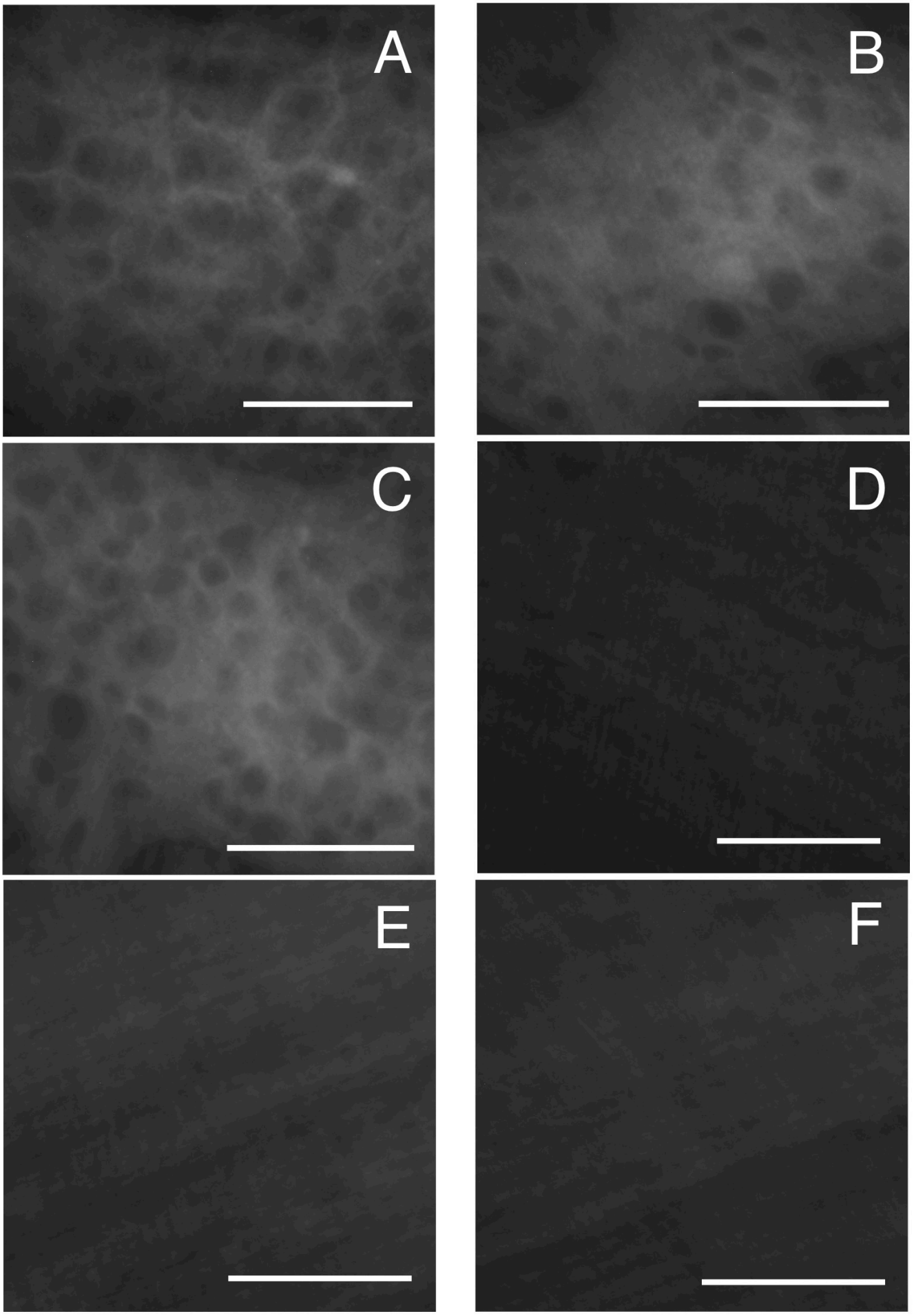
A
B
C
D
E
F

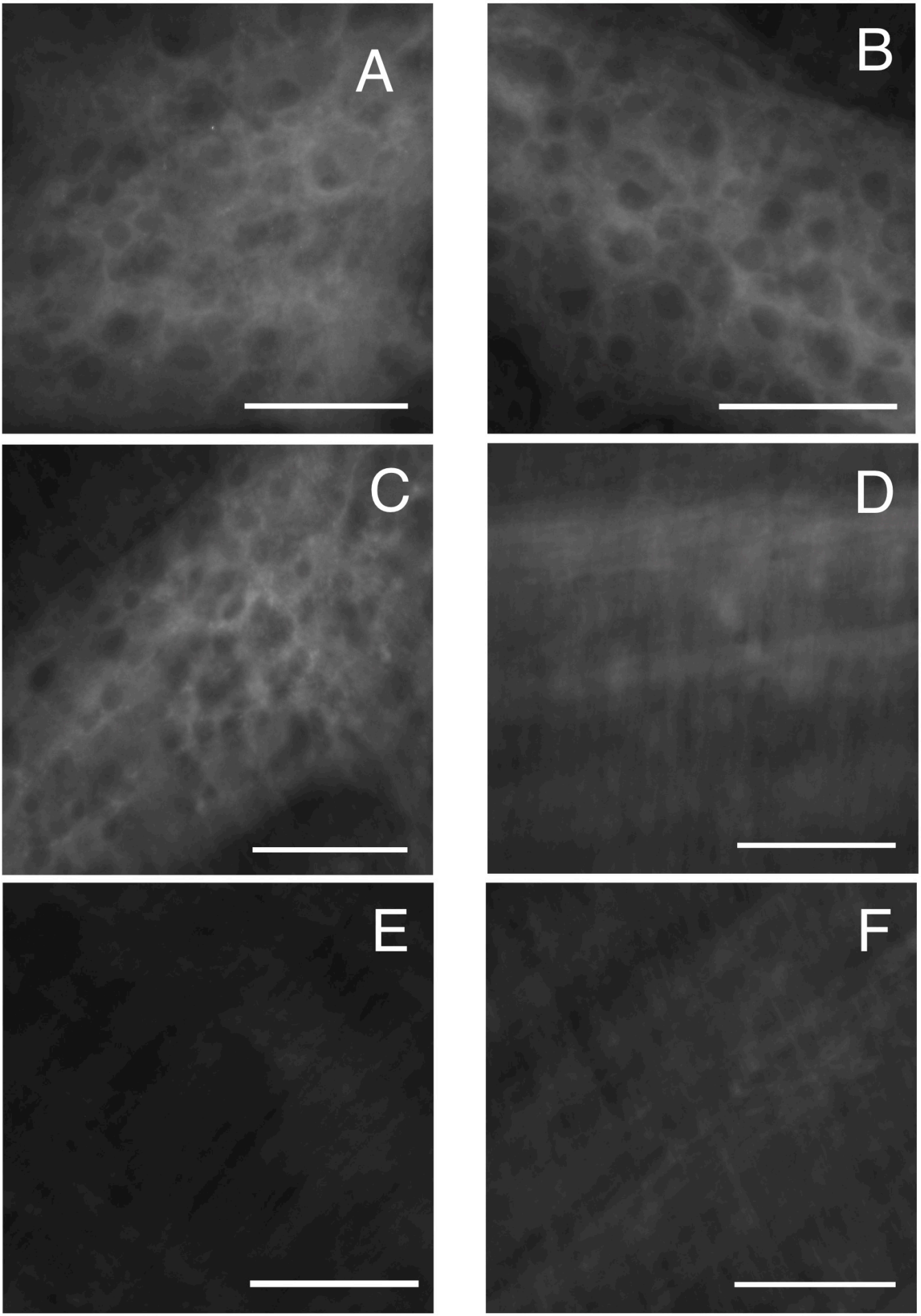
A
B
C
D
E
F

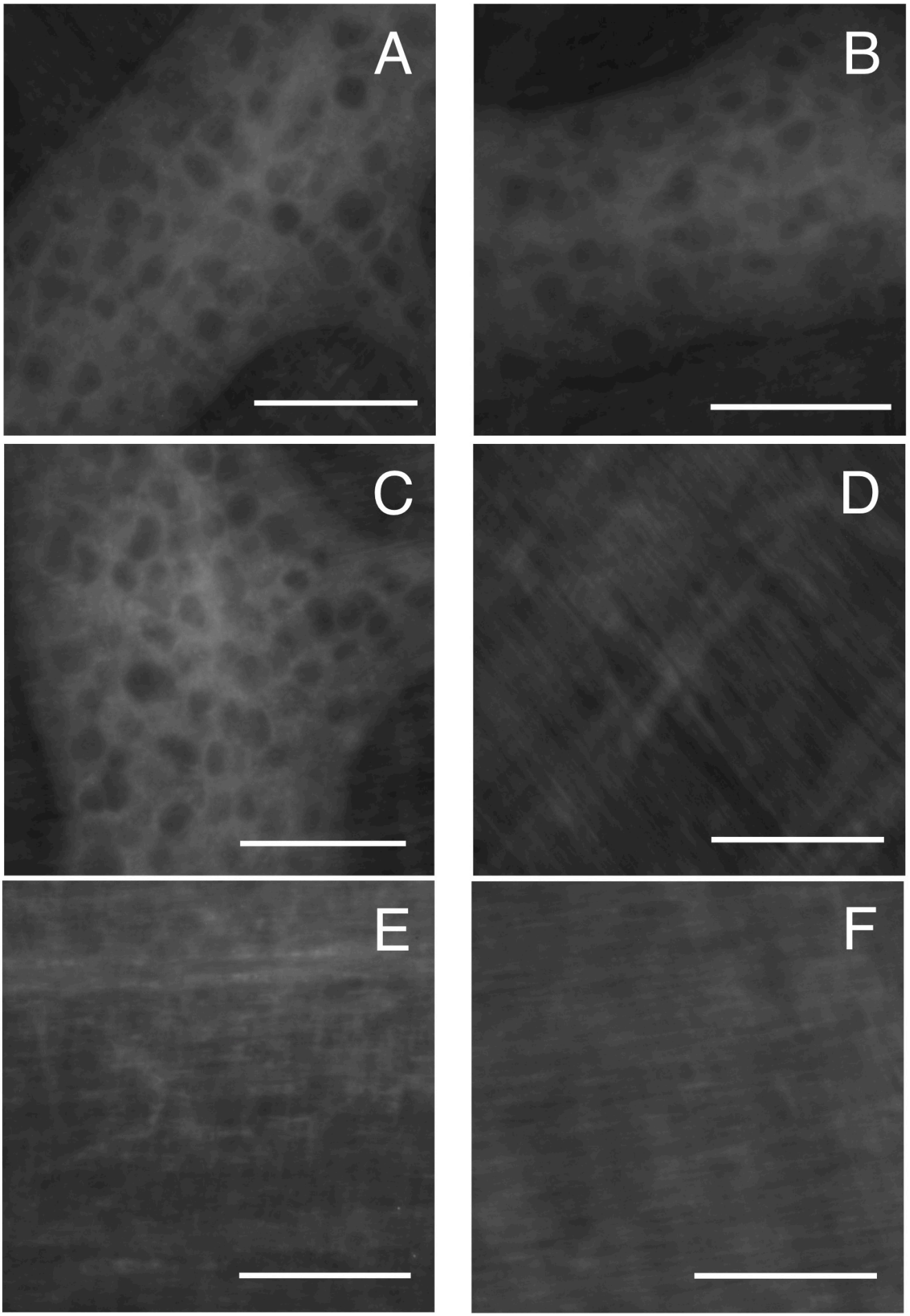
A
B
C
D
E
F

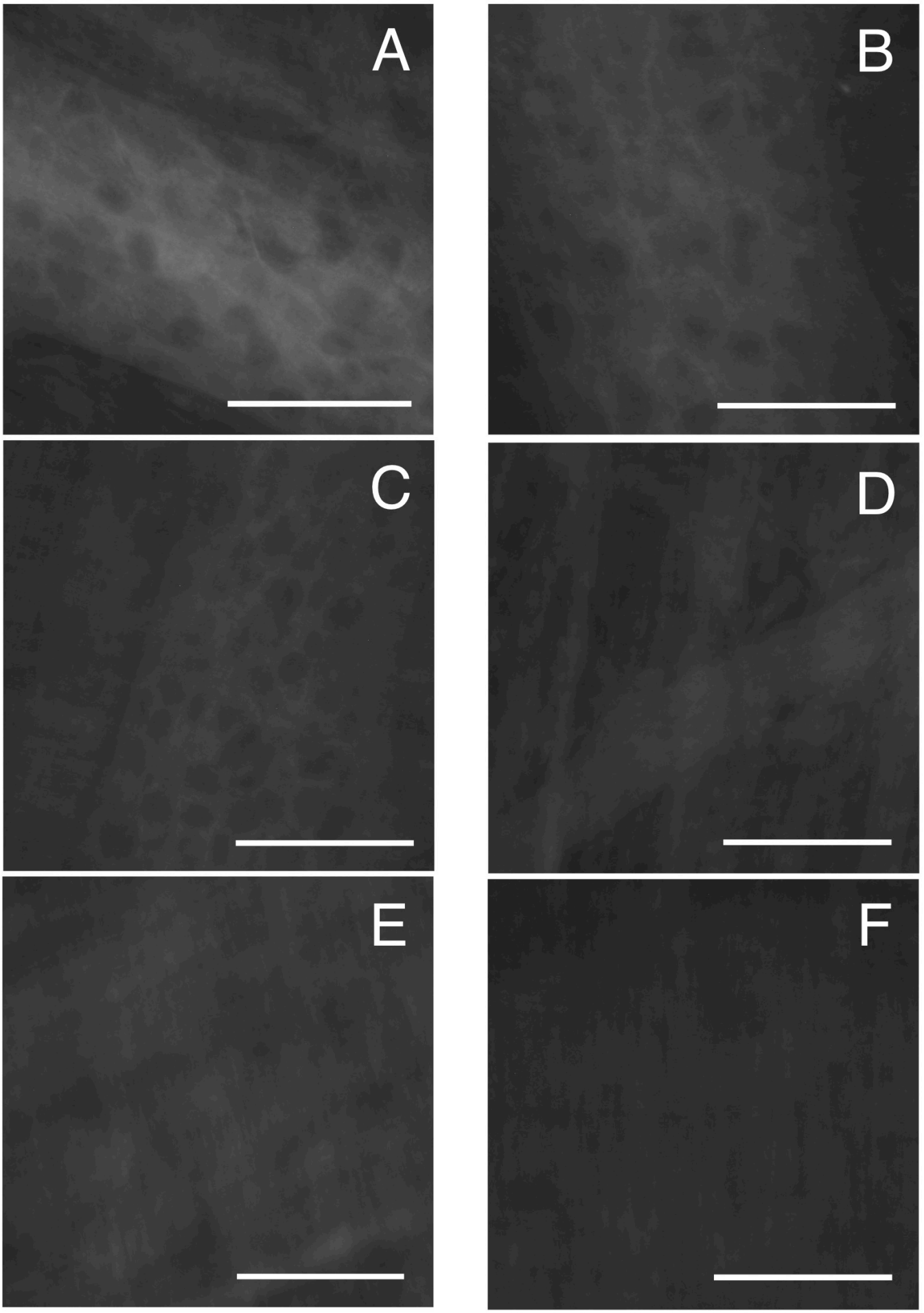
A
B
C
D
E
F

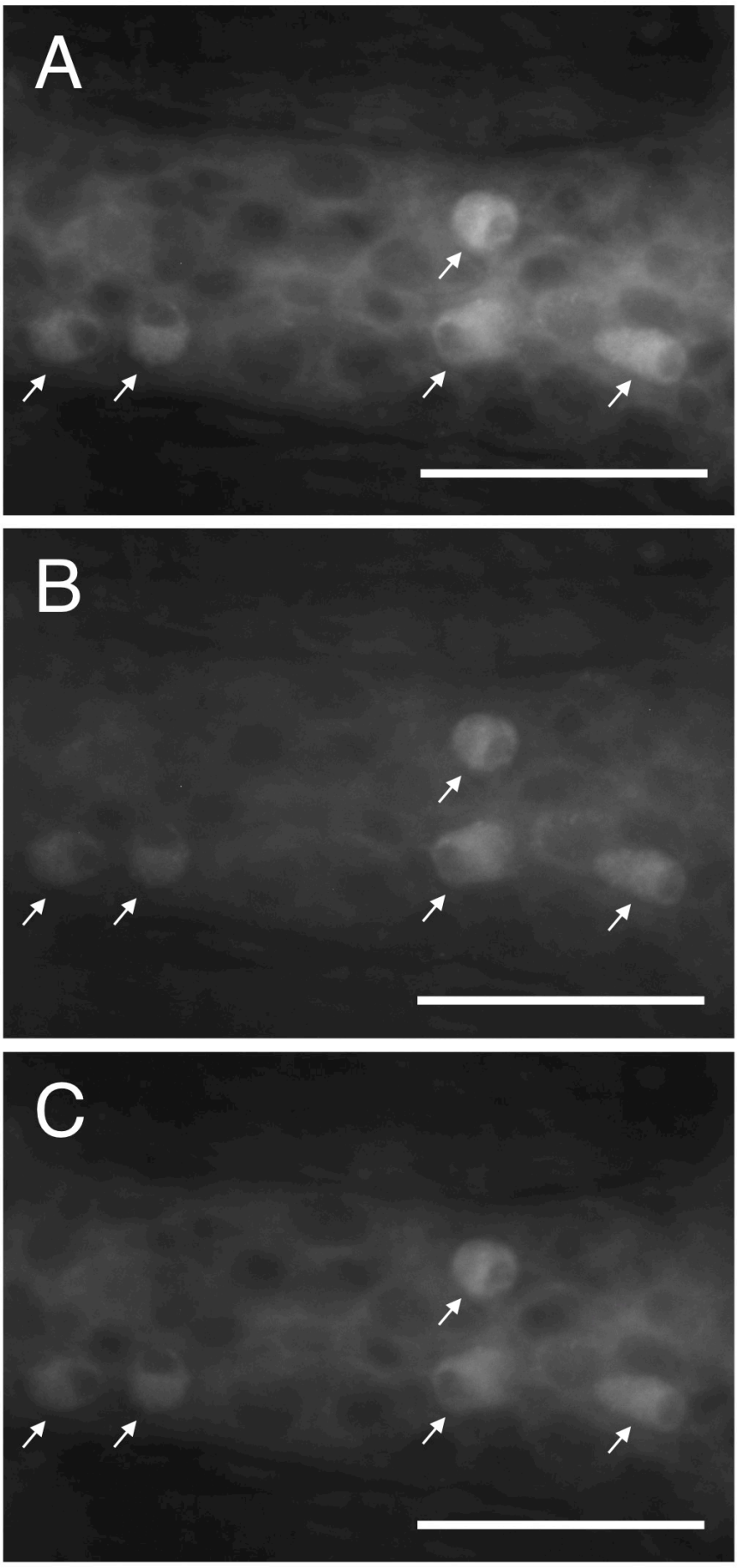
A
B
C

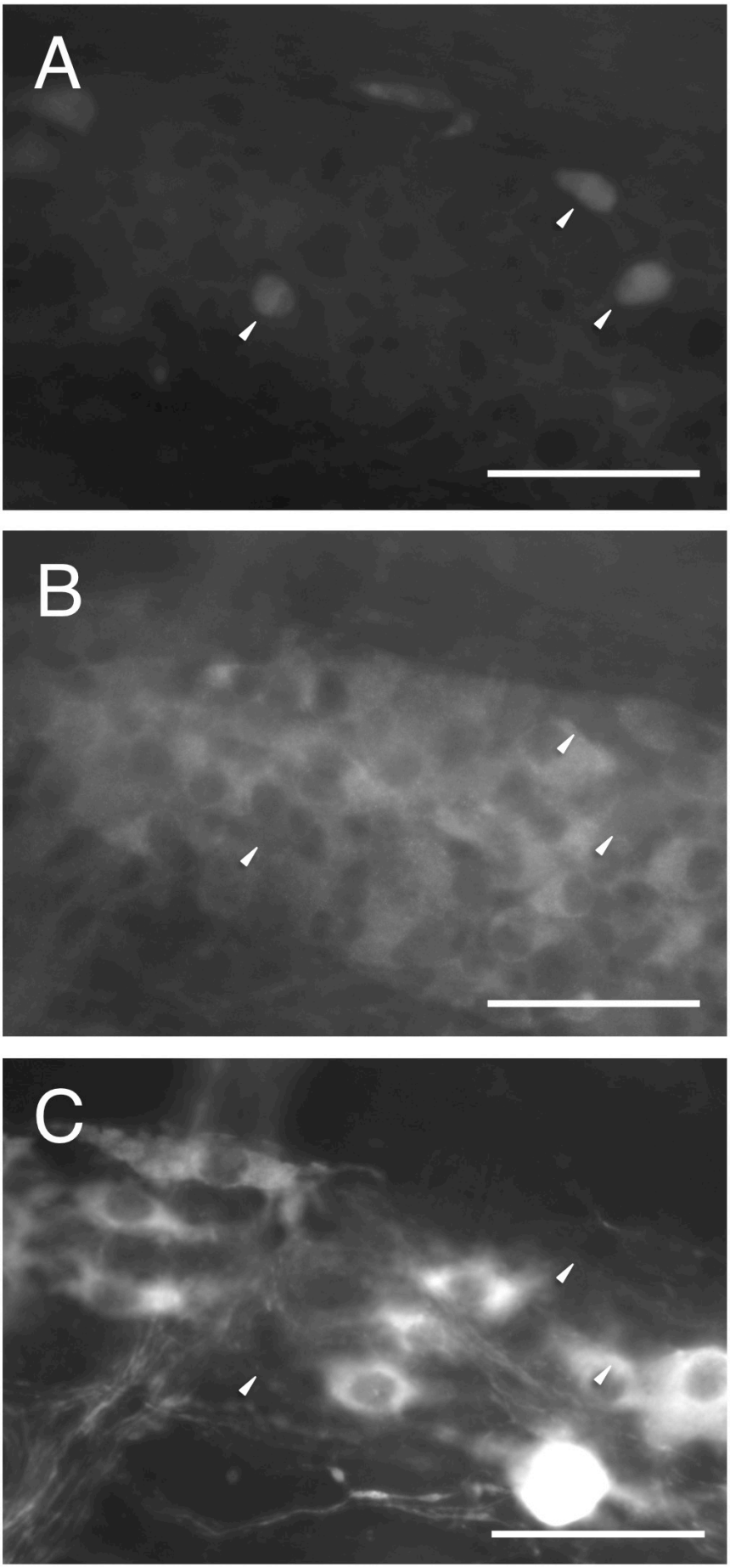
A
B
C

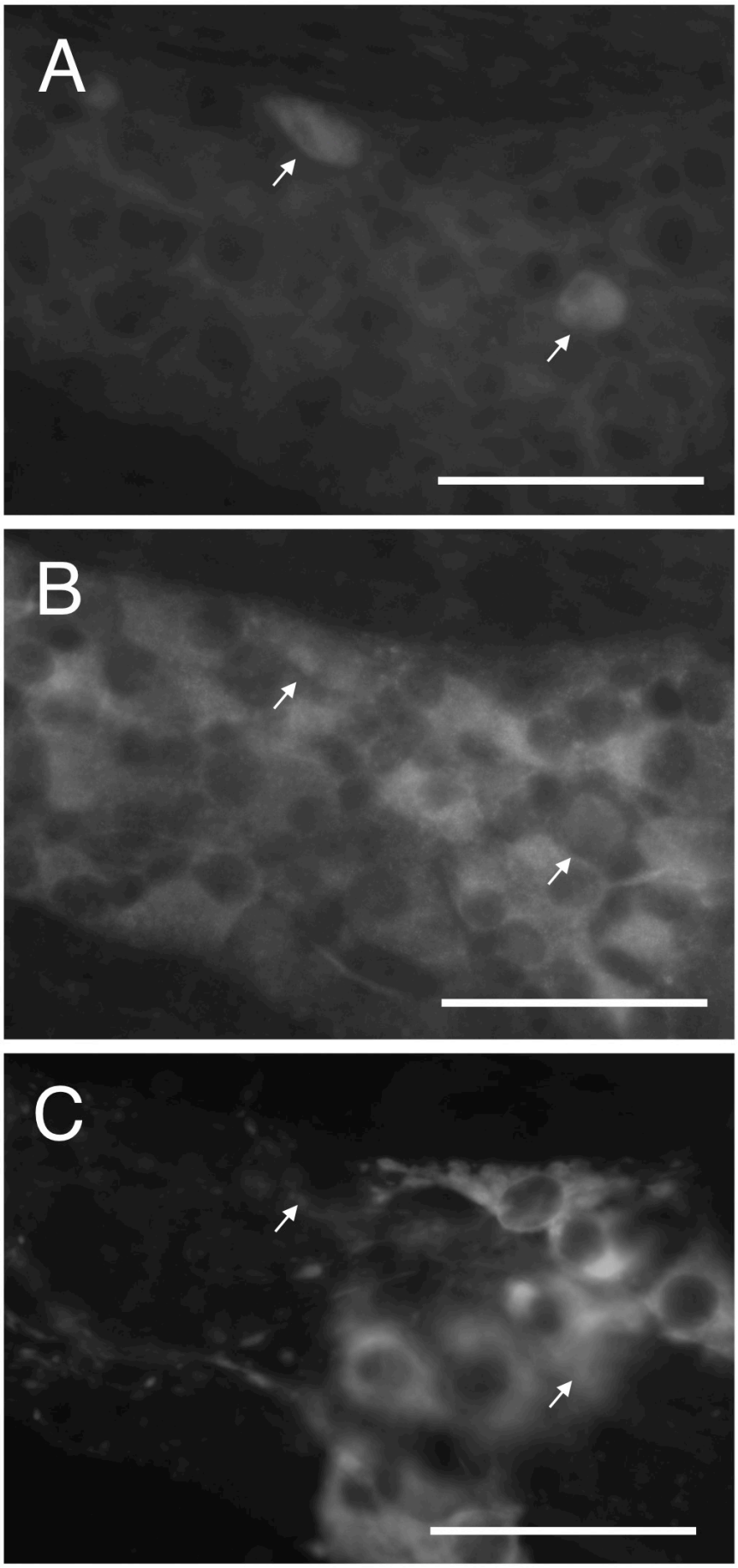
A
B
C

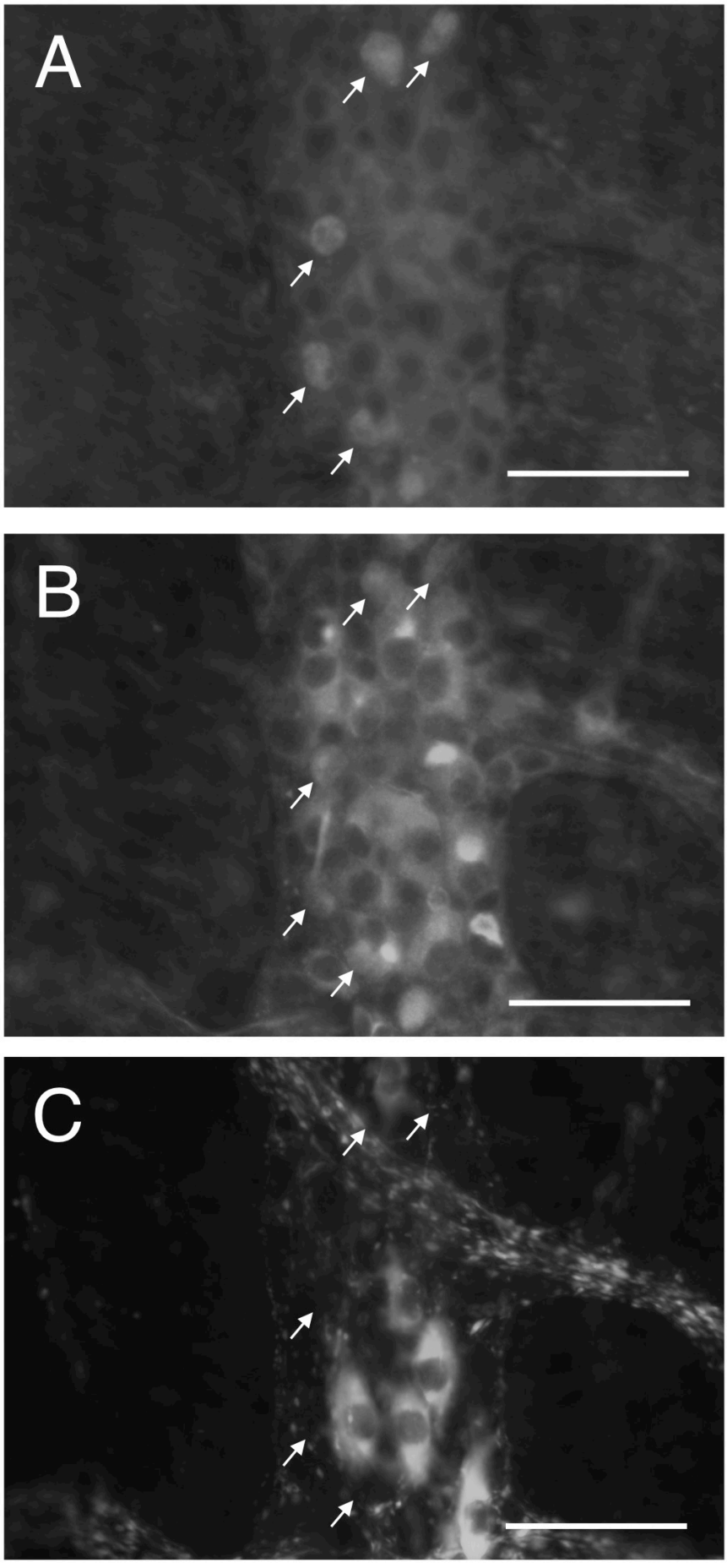
A
B
C

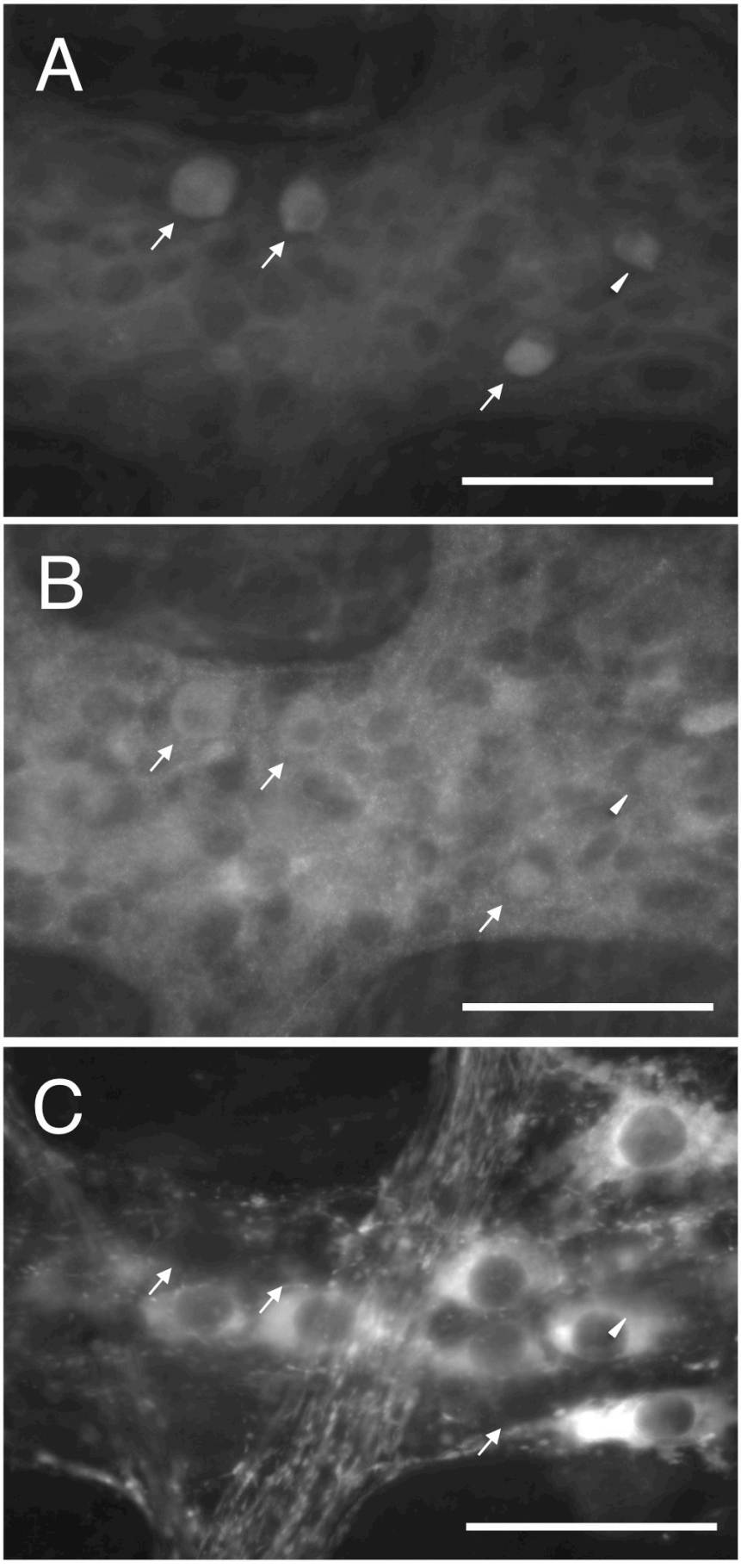
A
B
C